AD_____

Award Number: DAMD17-99-1-9352

TITLE: University of Pittsburgh Graduate Training Program in Breast Cancer Biology and Therapy

PRINCIPAL INVESTIGATOR: Olivera J. Finn, Ph.D.

CONTRACTING ORGANIZATION: University of Pittsburgh
Pittsburgh, Pennsylvania 15260

REPORT DATE: September 2002

TYPE OF REPORT: Annual Summary

PREPARED FOR: U.S. Army Medical Research and Materiel Command
Fort Detrick, Maryland 21702-5012

REPORT DOCUMENTATION PAGE

Form Approved
OMB No. 074-0188

1. AGENCY USE ONLY (Leave blank)	2. REPORT DATE	3. REPORT TYPE AND DATES COVERED
	September 2002	Annual Summary (1 Sep 01 - 31 Aug 02)

4. TITLE AND SUBTITLE
University of Pittsburgh Graduate Training Program in Breast Cancer Biology and Therapy

5. FUNDING NUMBERS
DAMD17-99-1-9352

6. AUTHOR(S)
Olivera J. Finn, Ph.D.

7. PERFORMING ORGANIZATION NAME(S) AND ADDRESS(ES)

University of Pittsburgh
Pittsburgh, Pennsylvania 15260

E-Mail: ojfinn@pitt.edu

8. PERFORMING ORGANIZATION REPORT NUMBER

9. SPONSORING / MONITORING AGENCY NAME(S) AND ADDRESS(ES)

U.S. Army Medical Research and Materiel Command
Fort Detrick, Maryland 21702-5012

10. SPONSORING / MONITORING AGENCY REPORT NUMBER

11. SUPPLEMENTARY NOTES
Original contains color plates: All DTIC reproductions will be in black and white.

12a. DISTRIBUTION / AVAILABILITY STATEMENT

Approved for Public Release; Distribution Unlimited

12b. DISTRIBUTION CODE

13. ABSTRACT ***(Maximum 200 Words)***

Our **Graduate Training Program in Breast Cancer Biology and Therapy** is a multidisciplinary approach focused on an important disease. The overall philosophy of our training program is to identify qualified graduate students in the existing discipline-based training programs and to interest and educate them in the unsolved problems in breast cancer.

The specific goals of our Program are: **a)** To recruit qualified predoctoral students to breast cancer related research; **b)** To educate students in the fundamental principles of breast cancer pathobiology and therapy; **c)** To monitor and evaluate the progress of the enrolled students and mentor them in their future career choices; **d)** To organize program activities, such as Seminar Series and Journal Clubs, for increased interaction of the student trainees with postdoctoral fellows and faculty interested in breast cancer.

We have completed the third year of the training program in which we have closely followed our specific goals. Six new students were selected for support in the years 3. One has graduated and a new student started her fellowships on September 1, 2001. Five students have made satisfactory progress in the first year of the award and have been awarded second year funding.

14. SUBJECT TERMS
breast cancer, graduate students, doctoral thesis, genetics, therapy

15. NUMBER OF PAGES
43

16. PRICE CODE

17. SECURITY CLASSIFICATION OF REPORT	18. SECURITY CLASSIFICATION OF THIS PAGE	19. SECURITY CLASSIFICATION OF ABSTRACT	20. LIMITATION OF ABSTRACT
Unclassified	Unclassified	Unclassified	Unlimited

Table of Contents

INTRODUCTION

Our **Graduate Training Program in Breast Cancer Biology and Therapy** is a multidisciplinary approach focused on an important disease. The overall philosophy of our training program is to identify qualified graduate students in the existing discipline-based training programs and to interest and educate them in the unsolved problems in breast cancer. By raising their interest and providing them with financial help, we encourage them to apply the tools of their individual disciplines in search of solutions to breast cancer-related problems. Our Training Program intends to expand the existing pool of investigators studying breast cancer. The Program also strives to encourage many of our faculty members, by including them into the list of Program Faculty and by providing support for their graduate students, to focus their research effort at least in part on breast cancer. This is an important programmatic by-product because it takes ongoing interdisciplinary research effort by an array of well-funded investigators and directs it towards the problems of breast cancer.

The specific goals of our Program are:

a) To recruit qualified predoctoral students to breast cancer related research.

b) To educate students in the fundamental principles of breast cancer pathobiology and therapy.

c) To monitor and evaluate the progress of the enrolled students and mentor them in their future career choices.

d) To organize program activities, such as Seminar Series and Journal Clubs, for increased interaction of the student trainees with postdoctoral fellows and faculty interested in breast cancer.

We have completed the third year of the training program in which we have closely followed our specific goals.

BODY (ANNUAL SUMMARY)

Progress in Trainee Recruitment

In the first two years of the grant we trained a total of seven students. Six were initially appointed and when two graduated in mid-year, several months earlier than expected, we funded one additional student for the last few months of his work before graduation, and awarded support to a new trainee. Of the total of eight trainees funded during the time covered by this progress report, 5 have obtained their PhD degrees, one is currently on the grant and two are continuing in their last year but funded by other sources. In 2001 we carried out nomination, competition and selection for the second group of trainees to be funded in the last two years of the grant. All training faculty, as well as the community at large, received an electronically transmitted letter informing them of the program and requesting trainee nominations. Applications were submitted also electronically and evaluated by the **Breast Cancer Training Grant Executive Committee**. The current committee members are Drs. Finn, Lazo, Morris and Latimer. Applicants were judged based on their performance in the first and second year of graduate school, faculty comments, and a brief written statement of their research interest as related to breast cancer. An effort was made to ensure equitable distribution of fellowships among multiple disciplines and areas of research. Five new students were selected to receive funding, four starting September 1, 2001 and the fifth January 1, 2002. In August 2002, one of our students graduated early and we awarded one year fellowship to a new student whose work will be described below.

Progress in Trainee Education and Monitoring of Progress:

Inasmuch as the students supported by this training grant belong to various graduate programs, the formal course work requirements and credits of dissertation research are determined by their individual programs. **The Training Program in Breast Cancer Biology and Therapy** requires that the students complete an Ethics course offered by the University and attend the weekly conference on Breast Cancer Biology and Therapy organized every Thursday afternoon by Dr. Jean Latimer. Each student is required to present a seminar in this series at least once during the two year period of support under the training grant..The Program Director, Dr. Finn, monitors all seminars campus wide and alerts the trainees to those of special interest to breast cancer.

Progress in Organizing Program Activities

In addition to several established seminar series that our trainees attend, the Magee Research Institute of the University of Pittsburgh and the University of Pittsburgh Cancer Institute Breast Program organized a series of monthly Debates on Breast Cancer Care which has now been named Seminars on Women's Health. Attendance is required of all the trainees.

Research Accomplishments of individual trainees from 9/1/2001 until 8/31/2002

Michel Gray (Dr. Sidney Morris, advisor), Molecular Biology Program. This student was awarded the fellowship starting 5/1/2001 and successfully defended his Ph.D. thesis in August 2002. His thesis was on the subject of arginases which are enzymes implicated in the enhanced proliferation rates of several types of cancers, including breast cancer, owing to their role in polyamine synthesis. In fact, inhibition of arginase activity in some human breast cancer cell lines results in inhibition of proliferation. Therefore, identification of the molecular mechanisms involved in regulation of arginase expression may provide new avenues for treatment of specific cancer types, including some forms of breast cancer. In particular, arginase expression is induced by a variety of cytokines and other inflammatory stimuli, suggesting that these agents may play a role in the onset and progression of cancer. As arginase expression is regulated primarily at the level of transcription, the specific aims of Michael Gray's project were to clone the promoters of the genes encoding the two arginase isozymes (types I and II), to map their transcription start sites, and to identify the DNA regulatory elements and transcription factors involved in induction of arginase I by IL-4 and cAMP and of arginase II by bacterial lipopolysaccharide (LPS) and cAMP. These objectives have been achieved and formed the basis for his Ph.D. dissertation, which was successfully defended on August 14, 2002. A portion of these results was presented at the Second International Conference on the Biology, Chemistry and Therapeutic Applications of Nitric Oxide in June, 2002. Two manuscripts describing this work are in preparation and will be submitted soon.

Publications:

Michael J. Gray and Sidney M. Morris, Jr. (2002) Regulation of Arginase I Transcription by IL-4 and cAMP in Murine Macrophages. Roles of SignalTransducer and Activator of Transcription-6, CCAAT Enhancer-binding Protein-ß, and Activator Protein-1. Submitted.

Abstracts:

S.M. Morris, Jr., and M. Gray (2002) Different transcription factors are required for induction of iNOS and arginase II by LPS. Nitric Oxide 6: 435-436.

Zoya Shurin (Dr. Paul Robbins, advisor), Bioengineering Graduate Program. Zoya has been supported for one year and her support was renewed for the second year. She works on the escape from immune surveillance as a fundamental feature of tumors, which contributes to their uncontrolled growth. The escape of malignant cells from immune recognition results from a defective function of cells of the immune system, including DC. CD40 plays an important role in both antitumor immunity and DC maturation. We have previously demonstrated that DC generated in vitro form bone marrow precursors obtained from tumor-bearers with MC38 colon adenocarcinoma have significantly lower expression of CD40 molecules compare to DC generated from tumor-free mice. In addition, levels of IL-12 production by these DC was lower then in tumor free controls, measured with and with out Staphylococcus aureus-induction. Recently, we showed that the same suppression of surface CD40 and IL-12 secretion observed in DC generated from tumor-bearing mice with TS/A breast adenocarcinoma. In addition we observed that levels of CD80 and CD86 are also decreased in these DC, compare to DC generated form tumor-free mice. The interaction between CD40 on antigen-presenting cells and its ligand CD40L (CD154) on T cells plays an important role in the induction of immune responses, including anti-tumor immunity. Soluble CD40L and transfer of the CD40L gene to tumor cells have been shown to induce specific immune responses in several murine tumor models. In her studies to date, Zoya, has evaluated whether expression of CD40L at the site of the tumor elicits an immune response to established tumors in mice. A recombinant adenovirus encoding murine CD40L (Ad-CD40L) was constructed and tested in the TS/A breast adenocarcinoma model. Administration of Ad-CD40L on Day 7 after tumor inoculation resulted in a significant inhibition of tumor growth when compared with the control groups treated with either saline or control adenovirus. She has examined the therapeutic efficacy of intratumoral injection of murine bone marrow-derived dendritic cells (DC) transduced with adenovirus encoding the CD40L. Intratumoral injection of DC/CD40L resulted in the majority of the animals being tumor-free 20 days post-therapy which was associated with induction of systemic immunity. Moreover, she

has demonstrated that DC overexpressing CD40L have no direct effect on TS/A breast adenocarcinoma cells in vitro, suggesting that DC/CD40L induced a specific antitumor response in vivo. Interestingly, DC/CD40L produced significantly higher levels of IL-12 than control DC, suggesting additional pathways of the antitumor activity of DC/CD40L. Her data demonstrate that Ad-CD40L transduction of DC or tumor cells at the site of the tumor may be an effective approach to induce an antitumor immune response to breast cancer.

Publications:

1 Shurin M.R., **Yurkovetsky Z.R.**, Barksdale E. Jr., Shurin G.V. Inhibition of CD40 expression during dendropoiesis by tumor: Role of GM3 and IL-10. Submitted.

2 Tourkova I.L., **Yurkovetsky Z.R.**, Gambotto A., Shurin M.R., Shurin G.V. Increased Function and Survival of IL-15-transfected Human Dendritic Cells are Mediated by Up-regulation of IL-15Rα and Bcl-2. Submitted.

3 Satoh Y., Esche C., Gambotto A., Shurin G.V., **Yurkovetsky Z.R.**, Robbins P.D., Watkins S.C., Todo S., Lotze M.T., Herberman R.B., Shurin M.R. Local Administration of IL-12-transfected Dendritic Cells Induces Antitumor Immune Responses to Colon Adenocarcinoma in the Liver in Mice. *J. Exp. Therap. Oncol.* In press.

4 Yamabe K., Peron J.M., Esche C., **Yurkovetsky Z.R.**, Watkins S., Lotze M.T., Shurin M.R. Lymphoid and myeloid dendritic cells: Functional differences between in vivo and in vitro generated cells. Submitted.

Abstracts:

1. **Yurkovetsky Z.R**, Gambotto A., Kim S.H., Shurin M.R., Robbins P.D. Intratumoral administration of Ad-CD40L or DC/CD40L elicited effective antitumor immunity in mice. 13th annual Virology Symposium, 2002.
2. **Yurkovetsky Z.R.,** Robbins P.D. Antitumor effect of adenoviral vectors expressing CD40L, RANKL or 4-1BBL. ASGT 5th annual meeting, 2002.
3. Kin S.H., **Yurkovetsky Z.R.,** Robbins P.D. Combined immunotherapy of a murine mammary tumor using genetically modified dendritic cells. ASGT 5th annual meeting, 2002.
4. **Yurkovetsky Z.R.,** Robbins P.D. Antitumor effect of adenoviral vectors expressing CD40L, RANKL or 4-1BBL. MGB retreat, 2002.
5. **Yurkovetsky Z.R.**, Shurin M.R., Robbins P.D. Intratumoral administration of adeno CD40L or dendritic cells overexpressing CD40L elicited effective antitumor immunity in mice. Era of Hope, DOD breast cancer research program meeting, 2002

Serkan Alkan (Dr. Christine Milcarek, advisor), Biochemistry and Molecular Genetics Program. Serkan has been funded for one year and his finding was renewed for another year. He works on the influence of hnRNP F and H on gene expression. The nuclear RNA binding proteins hnRNP F and H' have been shown to influence mRNA processing in many studies. The hnRNP F competes with polyadenylation factors and negatively influences expression. I am pursuing the mechanism of action of these proteins on cancer and differentiated cell products. By using RNA electromobility shift assays, he narrowed down the binding region of hnRNP F and H' on SV 40 late pre-mRNA to a 14 nucleotide Guanine rich region. Using serial RNA mutation analyses he concluded that the five consecutive Guanines in the sequence are necessary and sufficient for efficient hnRNP F and H' binding. He also verified that this binding is a result of specific RNA-protein interactions. Structure function analyses of hnRNP F will be conducted. He identified induced and repressed genes in murine plasmacytoma (AxJ) vs lymphoma cells (A20) by using microarray technology. He also did microarray analysis to compare the gene expression of hnRNP F, H' and empty vector transfected AxJ cells. He was looking for alternatively expressed and possibly polyadenylated genes using 12000 cDNAs as probes. He found many interesting genes, including plasmacytoma specific transcript 2 and lymphocyte specific transcript. The regulation of these will be pursued. He also found differential expression of mRNA for poly(A) binding protein II (PABII), which had been shown to be alternatively polyadenylated previously. Interestingly, PABII expression is *repressed* by 7 fold in AxJ cells compared to A20 cells. Overexpression of either hnRNP F or hnRNP H' releases this repression. He conclude that the hnRNP proteins F and H' can

influence gene expression and that their differential expression in a variety of tissues and cell states may be ubiquitous regulators of mRNA processing.

Meetings Attended:

1. Poster presentation at the 3' Processing meeting, Cold Spring Harbor NY, August 21-25 2001.
2. Poster presentation at the RNA Meeting, Wisconsin Madison May 28- June 2 2002.
3. Poster presentation at the DOD meeting in Orlando, September 2002.

Rafael Flores (Dr. Penelope Morell, advisor), Immunology Graduate Program. Rafael was funded for one year and his funding was just renewed for another year. A project that he has pursued this past year was the examination of the ability of murine bone marrow derived DCs to adopt either a DC1 or a DC2 functional phenotype. He conducted a preliminary study utilizing an *in vitro* protocol. Bone marrow cells from BALB/c mice were grown in GM-CSF for four days and then matured for 18 hours in the presence of TNF-a, PGE_2, or IL-4. Our results show that BM cells grown in GM-CSF and matured in the presence of TNF-a + PGE_2 were high producers of IL-12p70 whereas IL-4 matured DCs were low producers of IL-12p70. In addition to the high IL-12p70 production, the TNF-a + PGE_2 matured DCs exhibited a significantly higher level of CD86 than DCs matured with any other cytokine combination of cytokines. This pattern was also observed in experiments conducted with the BM cells of C57BL/6 and the NOD. In each mouse strain tested, IL-4 matured DCs were low producers of IL-12p70. Presently, he is analyzing the T cell polarizing ability of the different DC subsets. This work has importance fo induction of immune responses against tumors.

Meetings Attended

2002 FASEB-AAI Conference- Abstract Title "In Vitro Generation of Murine Bone Marrow Derived Dendritic Cell Types 1 and 2" Poster Presentation.

Nehad Alajez (Dr. Olivera J. Finn, advisor), Immunology Graduate Program. Nehad was funded for one year and his finding was extended for another year. He works on immunogenethrapy of breast cancer. MUC1 glycoprotein is overexpressed on the surface of a variety of epithelial tumors, most notably breast cancer, and has been under investigation as a target for immunotherapy. Cytotoxic T cell clones were generated from cancer patients that recognized MUC1 on the surface of tumor cells in an MHC-unrestricted manner. The T cell receptor (TCR) was cloned from one such clone (MA) and a two-chain (tc) and single-chain (sc) constructs were successfully expressed on the surface of a variety of cell lines. A secreted form of the scTCR receptor was expressed in 293 cells. Our Preliminary biacore data demonstrated the interaction between scTCR and tumor MUC1.The function of the scTCR was tested in vivo when a group of SCID mice were reconstituted with BM cells transduced with the scTCR amphotropic retroviral supernatant and challenged with MUC1-expressing human tumor cell lines. Tumor growth in mice reconstituted with TCR-transduced BM cells was significantly slower than that seen in the control group. The safety and efficacy of this approach are being tested in MUC1 transgenic mice. This strategy represents potentially efficacious gene therapy/immunotherapy for MUC1-expressing breast cancers. A non-MHC restricted TCR will make this treatment applicable to all cancer patients regardless of HLA type.

Meetings attended:

1- Poster presentation at Experimental Biology meeting, New Orleans, Louisiana, April 20-24, 2002
Title: Cancer immunogene therapy using MUC1-specific MHC-unrestricted T cell receptor.

2- Platform and poster presentation at the Era of Hope meeting for the DOD Breast Cancer Research Program, Orlando, FL, September 25-28, 2002.
Title: Cancer immunogene therapy using MHC-unrestricted MUC1-specific T cell receptor.

Alexander Ducruet(John Lazo, advisor), Pharmacology Graduate Program. Alexander works on targeted drug therapy for breast cancer. Cdc25 dual specificity phosphatases regulate cell cycle progression. Mammalian cells encode 3 distinct Cdc25 isoforms, Cdc25A, B, and C, with differing specificity for their putative substrate, the cyclin-dependent kinases (cdks). Cdc25B and Cdc25C are essential for entry into and progression through mitosis; Cdc25A seems to be a major regulator of S phase entry. Cdc25A has oncogenic and anti-apoptotic activity and is overexpressed in numerous human tumors, including breast carcinomas. Because of the emerging role for Cdc25A in neoplastic transformation, considerable interest exists for generating Cdc25 inhibitors for therapeutic intervention. The regulation of Cdc25A activity, however, appears to be complex and is not well characterized. Cdc25A undergoes both positive and negative regulatory phosphorylations. For example, ionizing radiation or ultraviolet light exposure induce Cdc25A phosphorylation that targets it for degradation. Cdc25A can also be phosphorylated by Cdk2, Raf1, and Pim-1, resulting in increased phosphatase activity. Treatment of human tumor cells with the cdk inhibitor roscovitine (10 μM for 24 hr) resulted in a 3-fold increase in Cdc25A protein levels in HeLa cervical carcinoma cells and a 5-fold increase in Cdc25A protein levels in MCF-7 breast adenocarcinoma cells. Similarly, a 24 hr treatment of HeLa cells with 100 μM olomucine, a structurally related cdk inhibitor with reduced potency, increased Cdc25A levels 3-fold. Further examination revealed that Cdc25A protein levels were affected in a concentration- and time-dependent manner, increasing as early as 30-60 min following compound exposure. Roscovitine treatment had no effect on Cdc25C levels and little to no effect on Cdc25B levels. A genetic approach was employed to determine the cdk activity that was responsible for this effect. Transfection of HeLa cells with a dominant-negative Cdk2 increased Cdc25A levels while no increase was seen with either a dominant-negative Cdk1 or Cdk3. These results support the hypothesis that Cdk2-mediated phosphorylation of Cdc25A decreases Cdc25A protein stability. Cdks are attractive therapeutic targets and cdk inhibitors are advancing into clinical trials. Nonetheless, the results suggest that elevated Cdc25A protein levels may be a potential negative side effect of Cdk2 inhibition, considering the oncogenic and anti-apoptotic potential of Cdc25A.

Publications

Lazo, J. S., Aslan, D. C., Southwick, E. C., Kooley, K. A., **Ducruet, A. P.**, Joo, B., Vogt, A. and Wipf, P. Discovery and biological evaluation of a new family of potent inhibitors of the dual specificity protein phosphatase Cdc25. *J. Med. Chem.* 44: 4042-4049, 2001.

Lyon M. A., **Ducruet, A. P.**, Wipf, P. and Lazo, J. S. Dual specificity phosphatases as targets for antineoplastic agents. *Current Topics in Medicinal Chemistry* **(In Press, 2002)**

Meetings

Gordon Research Conference on Chemotherapy of Experimental and Clinical Cancer, Colby-Sawyer College, New London, NH (July 14-19, 2002). Poster: Elevated Cdc25A Protein Levels in Response to Cyclin-Dependent Kinase Inhibition. Poster selected by attendees for informal oral presentation on final evening of conference)

Era of Hope Department of Defense Breast Cancer Research Program Meeting, Orange County Convention Center, Orlando, FL (September 25-28, 2002). Abstract Submitted: Elevated Cdc25A Protein Levels in Response to Cyclin-Dependent Kinase Inhibition. Abstract selected for Poster Presentation)

Jennifer Johnson (Jean Latimer, advisor), MD., PH.D. student, Biochemistry and Molecular Genetics Program. Jennifer is the newest student having just started on the grant in August 2002. She will be working on the analysis of DNA repair gene function and expression in novel repair-deficient breast tumor cell lines. : In this study she will (1) determined the transcription-based repair capacity of DNA repair in explants derived from pre-and post-menopausal breast reduction tissue, Ductal Carcinoma *In Situ* (DCIS), and stage I and II tumors; (2) perform RNAse Protection Analysis (RPA) on the explants using 20 cloned NER genes from a commercially available kit on RNA derived from the same explants to identify candidate genes; (3) perform Real-Time PCR analysis and Western Blot analysis of the candidate genes to confirm their mRNA levels and determine the protein levels within these explants.

APPENDIX TO THE SUMMARY

1) Key research accomplishments:

- Promoters of the genes encoding two human arginase isozymes (types I and II) were cloned, their transcription start sites mapped, and the DNA regulatory elements and transcription factors involved in induction of arginase I by IL-4 and cAMP and of arginase II by bacterial lipopolysaccharide (LPS) and camp identified.
- A new anti-tumor therapy was identified based on DC/CD40L.
- A new set of genes was identified that are alternatively expressed and polyadenylated that may control cell differentiation.
- Additional characterization of dendritic cell subsets was obtained that can influence immune responses towards type 1 (protective from tumor) or type 2 (not protective).
- A new reagent was created for immunotherapy/gene therapy of breast cancer in the form of a retroviral vector expressing a tumor-specific T cell receptor.
- Further evaluation was performed on Cdk2 inhibitors for targeted tumor therapy, with the results bringing a cautionary note about potential negative side effects.

2) Reportable outcomes

- One trainee obtained his Ph.D. degree.
- Two papers were published, authored or co-authored by the trainees.
- One Ph.D. theses was published.
- Two papers are in press.

3) Three copies of the published papers are included.

Discovery and Biological Evaluation of a New Family of Potent Inhibitors of the Dual Specificity Protein Phosphatase Cdc25

John S. Lazo, Diana C. Aslan, Eileen C. Southwick, Kathleen A. Cooley, Alexander P. Ducruet, Beomjun Joo, Andreas Vogt, and Peter Wipf

Departments of Pharmacology and Chemistry, University of Pittsburgh, Pittsburgh, Pennsylvania 15260

JOURNAL OF
MEDICINAL CHEMISTRY®

Reprinted from
Volume 44, Number 24, Pages 4042–4049

Articles

Discovery and Biological Evaluation of a New Family of Potent Inhibitors of the Dual Specificity Protein Phosphatase Cdc25

John S. Lazo,*,† Diana C. Aslan,‡ Eileen C. Southwick,† Kathleen A. Cooley,† Alexander P. Ducruet,† Beomjun Joo,‡ Andreas Vogt,† and Peter Wipf‡

Departments of Pharmacology and Chemistry, University of Pittsburgh, Pittsburgh, Pennsylvania 15260

Received May 8, 2001

The Cdc25 dual specificity phosphatases have central roles in coordinating cellular signaling processes and cell proliferation, but potent and selective inhibitors are lacking. We experimentally examined the 1990 compound National Cancer Institute Diversity Set and then computationally selected from their 140 000 compound repository 30 quinolinediones of which 8 had in vitro mean inhibitory concentrations <1 μM. The most potent was 6-chloro-7-(2-morpholin-4-ylethylamino)quinoline-5,8-dione (NSC 663284), which was 20- and 450-fold more selective against $Cdc25B_2$ as compared with VHR or PTP1B phosphatases, respectively. NSC 663284 exhibited mixed competitive kinetics against Cdc25A, $Cdc25B_2$, and Cdc25C with K_i values of 29, 95, and 89 nM, respectively. As compared with NSC 663284, the regioisomer 7-chloro-6-(2-morpholin-4-ylethylamino)quinoline-5,8-dione was 3-fold less active against $Cdc25B_2$ in vitro and less potent as a growth inhibitor of human breast cancer cells. Computational electrostatic potential mapping suggested the need for an electron-deficient 7-position for maximal inhibitor activity. Using a chemical complementation assay, we found that NSC 663284 blocked cellular Erk dephosphorylation caused by ectopic Cdc25A expression.

Introduction

Reversible protein phosphorylation is a ubiquitous intracellular process required for mammalian cell communication and growth. Determined by the dynamic balance between protein kinases and phosphatases, serine, threonine, or tyrosine phosphorylation can affect catalytic activity or promote protein−protein interactions that influence subcellular location and functionality. Small molecule inhibitors have provided valuable tools to decode the role of kinases and phosphatases participating in specific cellular signaling pathways, because they are generally reversible and readily enter cells. Natural product inhibitors of serine/threonine protein phosphatases, such as okadaic acid and calyculin A, have been extremely valuable reagents to probe serine/threonine phosphatase function; there is however an absence of potent and selective inhibitors for the other major mammalian phosphatase class, namely, the protein tyrosine phosphatases (PTPase), which includes the dual specificity protein phosphatase (DSPase) subfamily. The PTPases are defined by the active site signature sequence motif HCX_5R, where H is a highly conserved histidine residue, C is the catalytic cysteine, the five X residues form a loop in which all of the amide nitrogens hydrogen-bond to the phosphate of the substrate, and R is a highly conserved arginine that hydrogen bonds to the phosphorylated amino acid of the substrate.[1] While the DSPases retain the conserved HCX_5R motif, they are unique in their ability to hydrolyze both phosphoserine/threonine and phosphotyrosine residues on the same protein substrate.[1] Important members of the DSPase family are the Cdc25 phosphatases, which control cell cycle progression by activating cyclin-dependent kinases (Cdk)[2] and participate in Raf-1-mediated cell signaling.[3]

Three Cdc25 homologues exist in humans: Cdc25A, Cdc25B, and Cdc25C.[2,4−6] Cdc25A and B have oncogenic properties,[7] are transcriptional targets of the c-*myc* oncogene,[8] and are overexpressed in many human tumors.[9,10] Both Cdc25B and Cdc25C are thought to be regulators of G2/M transition through their ability to dephosphorylate and activate the Cdk1/cyclin B mitotic kinase complex, which is required for cell entry into mitosis.[2,11] Cdc25A is likely to be important for G1/S phase transition and in preserving genomic integrity,[12−14] although Cdc25A may also have some role in the initiation of mitosis.[14] Cdc25A is rapidly degraded in response to DNA damage, which impairs the G1/S transition.[15] Cdc25A may also have other cellular roles as it has been shown to regulate the tyrosine phosphorylation status and kinase activity of Raf-1, which has a central role in the mitogen-activated kinase signal transduction pathway.[3]

Although two crystal structures have been published for the Cdc25 catalytic domain,[16,17] none expose the nature of interactions with small molecule inhibitors. Moreover, the protein substrate may initiate key conformational changes and provide an important catalytic acid.[18,19] Thus, rational design parameters for potential inhibitors are lacking. The current work was initiated

* Corresponding author telephone: (412)648-9319; fax: (412)648-2229; e-mail: lazo@pitt.edu.
† Department of Pharmacology.
‡ Department of Chemistry.

10.1021/jm0102046 CCC: $20.00
Published on Web 10/18/2001

Table 1. Chemical Structures of Quinolinedione Cdc25 Inhibitors and In Vitro Activity against Recombinant Human $Cdc25B_2$, VHR, or PTP1B[b]

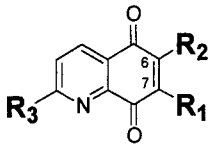

NSC	R_1	R_2	R_3	IC_{50} (μM) Cdc25	VHR	PTP1B
668394	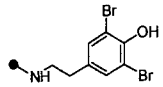	H	H	0.64 ± 0.13	8.5[a]	8.0[a]
663284	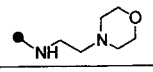	Cl	H	0.21 ± 0.08	4.0 ± 0.1	> 100
45384	NH	OMe	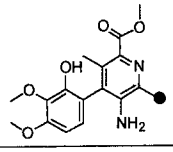	0.37 ± 0.08	5.1 ± 0.1	8.7 ± 0.3
677948	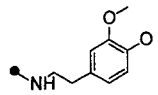	H	H	0.45 ± 0.02	17 ± 0.5	> 100
677949	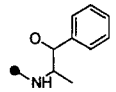	H	H	0.51 ± 0.01	16 ± 2.0	>100
677945	H	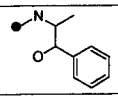	H	0.67 ± 0.04	>10	>10
663282	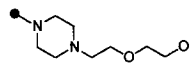	Cl	H	0.90[a]	>10	>10
662383	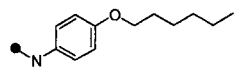	Cl	H	0.93[a]	>10	>10

[a] Single determination. [b] IC_{50} values were from 3 or more determinations with SEM indicated.

based on the belief that selective Cdc25 inhibitors could be obtained by using a general and unbiased approach to evaluate a chemically diverse compound library. Thus, we probed a small subset of the National Cancer Institute's (NCI) 140 000 compound library for a potential inhibitory pharmacophore and used this information to identify a pharmacophore yielding the most potent and selective inhibitor of Cdc25 reported to date. This compound had marked antiproliferative activity against human tumor cells and blocked the biochemical actions of ectopic Cdc25A expression.

Results

Quinolinediones from the NCI Compound Library Inhibited Human Cdc25. Initially, we examined the 1990 compounds comprising the NCI Diversity Set, which was designed to be representative of the 140 000 NCI compound repository. Members of the Diversity Set have been evaluated by the NCI for growth inhibition against the NCI 60 Tumor Cell Panel, and these data are publicly available at http//www.dtp.nci.nih.gov/. We examined the Diversity Set for in vitro inhibition of recombinant full-length human $Cdc25B_2$ and found 24 compounds that caused >80% inhibition at 10 μM. Upon reevaluation, 5 of the 24 compounds had IC_{50} values <1 μM; the most potent $Cdc25B_2$ inhibitor was the quinolinedione NSC 668394, which had an IC_{50} of 640 ± 130 nM against $Cdc25B_2$ and had ≥8-fold preference for $Cdc25B_2$ as compared to the DSPase VHR or the PTPase PTP1B (Table 1). Moreover, the mean IC_{50} for growth inhibition by NSC 668394 was 2.1 ± 2.0 μM when assayed in the NCI 60 Tumor Cell Panel (see http://www.dtp.nci.nih.gov/). NSC 668394 was the sole quinolinedione in the Diversity Set. The importance of the 5,8-dione pharmacophore for Cdc25 inhibition was emphasized by the lack of significant anti-phosphatase activity at 10 μM with any of the other 118 quinoline structures evaluated in the Diversity Set. To test the hypothesis that the quinolinedione pharmacophore was important for Cdc25 inhibitory activity, Jill Johnson (NCI, Developmental Therapeutics Program, Rockville, MD) computationally identified 30 additional quinolinediones in the NCI Compound Repository, and we examined them experimentally for anti-phosphatase activity. When tested, all of these compounds had in vitro IC_{50} values <40 μM for $Cdc25B_2$, and seven had IC_{50} values <1 μM. The mean IC_{50} value was 5.4 ± 1.5 μM. Six of the seven most active compounds were

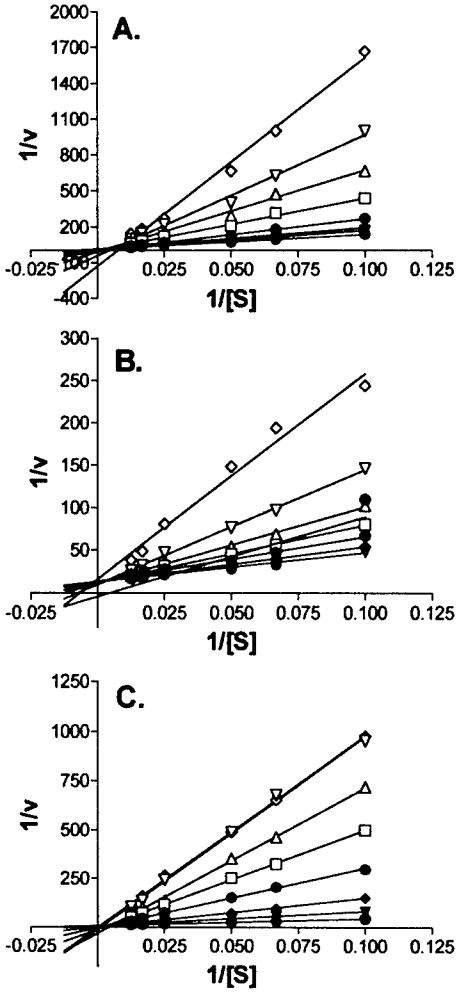

Figure 1. Lineweaver–Burk plots for NSC 663284 inhibition of Cdc25 isoforms. (A) Cdc25A. Concentrations of NSC 663284 are ▼, 15; ◆, 25; ●, 50; □, 100; △, 150; ▽, 200; ◇, 300 nM. (B) $Cdc25B_2$, ▼, 25; ◆, 50; ●, 100; □, 150; △, 200; ▽, 300; ◇, 500 nM. (C) Cdc25C. ▼, 25; ◆, 50; ●, 100; □, 150; △, 200; ▽, 300; ◇, 500 nM.

7-substituted quinolinediones, with the most potent (NSC 663284) having an IC_{50} value of 206 ± 75 nM (Table 1). All of the submicromolar inhibitors displayed a strong preference for $Cdc25B_2$ as compared with VHR or PTP1B. For example, with NSC 663284, the relative IC_{50} values for $Cdc25B_2$ were 20- and 450-fold lower than for VHR or PTP1B, respectively.

We examined further the kinetics and relative sensitivity of each of the full-length human Cdc25 isoforms to NSC 663284. For all three Cdc25 isoforms, NSC 663284 inhibition kinetics fit best to a partial mixed competitive model, which may reflect the potential for interactions at the two anionic binding sites as observed in the crystal structure of Cdc25B[17] (Figure 1). The calculated K_i values for Cdc25A, Cdc25B, and Cdc25C were 29 ± 7, 95 ± 14, and 89 ± 18 nM (n = 4–6, ± SEM), respectively, suggesting that NSC 663284 had 3-fold selectivity toward Cdc25A as compared with either Cdc25B or Cdc25C.

Analogue Analyses Revealed the Importance of the C-7 Substitution for Potent Cdc25 Inhibition. To interrogate further the quinolinedione pharmacophore, we resynthesized NSC 663284, DA3003-1, and synthesized the regioisomer of NSC 663284, namely,

Table 2. Structures and Activity of Synthesized Heteroarenedione Analogues[b]

Name	Structure	IC_{50} (μM)		
		$Cdc25B_2$	VHR	PTP1B
DA3003-2	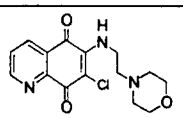	0.82 ± 0.08	>10	>10
DA276	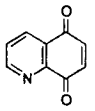	3.0 ± 1.4	>10	>10
DA3002	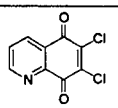	4.6 ± 1.0	>10	>10
DA3100	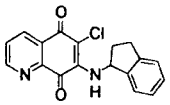	0.30 ± 0.03	ND	ND
DA3018	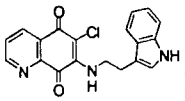	5.1 ± 0.6	>10	>10
DA3020	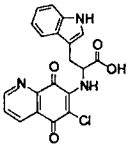	16 ± 4	>10	>10
DA295	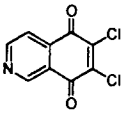	1.5 ± 0.7	>10	>10
DA3044	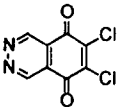	8.9 ± 5.0	>10	>10
DA3045	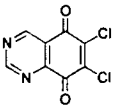	4.8 ± 2.8	>10	>10
DA296	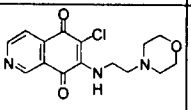	0.59 ± 0.18	>10	>10
DA3049	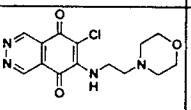	0.43 ± 0.03	1.1[a]	9.8[a]

[a] Single determination. [b] IC_{50} values were from 3 or more determinations with SEM indicated. ND = not determined.

DA3003-2, as well as several other analogues. A comparative study with the minimal quinolinedione, isoquinolinedione, phthalazinedione, and quinazolinedione (namely, DA276, DA3002, DA295, DA3044, and DA3045) revealed that a heterocyclic quinone pharmacophore alone was insufficient for potent Cdc25 inhibition (Table 2). NSC 663284 had identical inhibitory properties as compared to DA3003-1 against Cdc25A, Cdc25B, and Cdc25C as well as HPLC and spectral profiles. Thus, we used NSC 663284 for most of the subsequent biological studies because of the much greater quantities

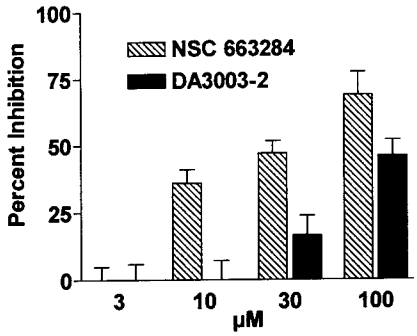

Figure 2. Growth inhibition of NSC 663284 and DA3003-2. Cells were treated for 3 h with NSC 663284 (hatched bars) or the regioisomeric DA3003-2 (black bars), and cell growth was determined 48 h later as described in the Experimental Section.

available to us. Addition of the 2-morpholin-4-ylethylamino moiety at the 7-position clearly enhanced inhibitory activity against Cdc25B as indicated by comparing the IC_{50} values of DA3049 with DA3044, of DA296 with DA295, or of NSC 663284 with either DA3002 or DA276. Other 7-substituted analogues, such as DA3018 and DA3020, were poor inhibitors of Cdc25B, although DA3100 exhibited significant inhibitory activity indicating that the 2-morpholin-4-ylethylamino moiety was one of at least two unique enhancers. For this limited series, the quinolinedione pharmacophore provided a superior scaffold as compared to the other heterocycles. Thus, the quinoline analogue NSC 663284 was a more potent inhibitor than either the isoquinoline analogue DA296 or the phthalazine analogue DA3049. The 7-substituted quinolinedione NSC 663284, which contained the 2-morpholin-4-ylethylamino moiety at the 7-position, was also approximately 3-fold better as an inhibitor of $Cdc25B_2$ than its regioisomer DA3003-2 and was the most potent inhibitor of all compounds tested.

NSC 663284 Blocked Cell Proliferation and the Actions of Cellular Cdc25A. NSC 663284 had a mean IC_{50} value in the NCI 60 Cell Human Tumor Panel of 1.5 ± 0.6 μM when cells were treated for 48 h. Most sensitive were human breast cancer MDA-MB-435 and MDA-N cells, which had IC_{50} values of 0.2 μM. We observed an IC_{50} for growth inhibition of 1.7 μM with continuous 48-h NSC 663284 treatment of human breast MCF-7 cells in culture (data not shown). Even after only a 3-h exposure to NSC 663284, we observed an IC_{50} for growth inhibition of ~35 μM with MCF-7 cells (Figure 2). Consistent with in vitro Cdc25 inhibition, the IC_{50} for growth inhibition after a 3-h exposure to NSC 663284 was 3-fold lower than that seen with the 6-regioisomer DA3003-2 (Figure 2). To probe for inhibition of cellular Cdc25 activity, we used a recently described chemical complementation assay,[20] which revealed the ability of a small molecule to complement or reverse a biochemical effect caused by ectopic Cdc25A expression. The advantage of this assay for studying small molecules that also may affect cell cycle progression is the requirement for only a brief exposure of an asynchronous cell population to an agent. Cdc25A has been implicated in controlling the phosphorylation status of Raf-1, which is a proximal effector of the mitogen-activated protein kinase (Erk1/2) pathway.[3] Thus, transient expression of full-length Cdc25A in

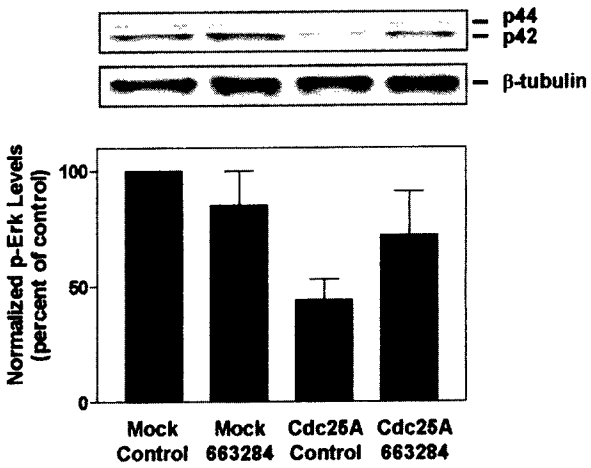

Figure 3. Reduction of phospho-Erk levels by Cdc25A overexpression and inhibition of Cdc25A activity by NSC 663284. (Upper Panel) Western blot of phospho-Erk levels after mock transfection (lanes 1 and 2) or wild-type human Cdc25A transfection (lanes 3 and 4). Cells were treated for 1 h with vehicle (lanes 1 and 3) or 10 μM NSC 663284 (lanes 2 and 4). (Middle Panel) β-tubulin was used as a loading control. (Lower Panel) Quantification of the phospho-Erk levels in cells after treatment with NSC 663284. $n = 4$; bars = SEM. Only Cdc25A control was less than mock control ($p < 0.05$, Student's t-test).

HeLa cells resulted in a >50% decrease in Erk phosphorylation (Figure 3). Treatment of mock (no Cdc25) transfected cells with 10 μM NSC 663284 caused no significant increase in Erk phosphorylation while exposure of Cdc25A transfected cells for 1 h to 10 μM NSC 663284 reversed the depression of Erk phosphorylation caused by Cdc25A transfection and returned phospho-Erk to constitutive levels (Figure 3). These results support the hypothesis that NSC 663284 blocked the biological effects of Cdc25A within cells.

The substitution with amino groups at 6- and 7-positions, respectively, of the quinone cores of NSC 663284 and DA3003-2 was significant for increasing inhibitory activity. This effect could be due to a polarization of the electron distribution in the quinolinedione, since the decrease in activity of the chlorinated derivative is considerable and the difference in activity between DA3100 and NSC 663284 was much less pronounced. The latter two compounds would be expected to exhibit a closely related electronic polarization of the quinone core. IC_{50} values of NSC 663284, NSC 668394, DA3100, DA296, DA3049, and DA3003-2 vary by a factor of 3, while IC_{50} values for the corresponding dichloro analogues DA3002, DA295, and DA3044 are about an order of magnitude higher. Electron density surfaces encoded with the electrostatic potential obtained by ab initio computation of the core pharmacophore structure demonstrate that, despite significant differences in the position and the number of nitrogen atoms, NSC 663284, DA296, DA3049, and DA3003-2 have closely related, polarized electron distributions (Figure 4). In comparison, the analogous graphs for dichloro analogues DA3002, DA295, and DA3044 show a very different, much less polarized electrostatic potential surface (Figure 5). On the basis of this analysis, it becomes clear that replacing a chloride substituent with an amino group leads to a considerable perturbation of the electron distribution in heteronaphthoquinones and that

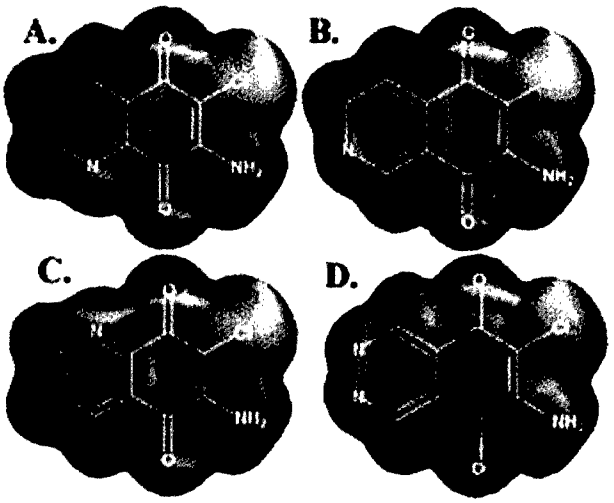

Figure 4. Electrostatic potential-encoded electron density surfaces of the core structures of NSC 663284 (A), DA296 (B), DA3003-2 (C), and DA3049 (D). The surfaces were generated with Spartan 5.1.1 (Wavefunction, Inc.) after ab initio minimization with a 3-21G* basis set. The coloring represents electrostatic potential with red indicating the strongest attraction to a positive point charge and blue indicating the strongest repulsion. The electrostatic potential is the energy of interaction of the positive point charge with the nuclei and electrons of a molecule. It provides a representative measure of overall molecular charge distribution.

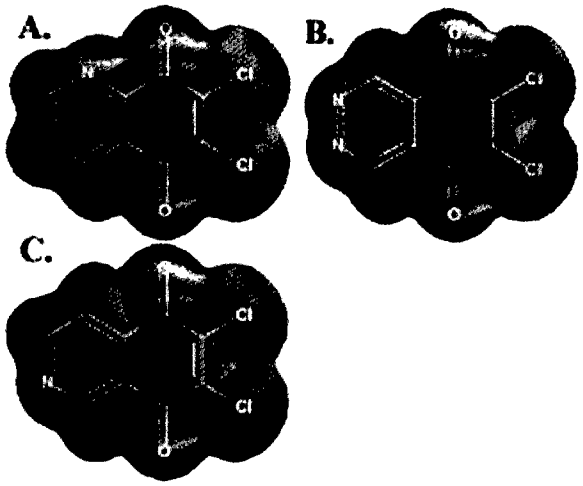

Figure 5. Electrostatic potential-encoded electron density surfaces of less active core structures: DA3002 (A), DA295 (B), and DA3044 (C). The surfaces were generated with Spartan 5.1.1 (Wavefunction, Inc.) after ab initio minimization with a 3-21G* basis set.

this electrostatic effect is likely to provide a better match for the complementary surface in the enzyme binding pocket. The core structure of NSC 663284 could therefore represent a general motif for the electronic configuration that is necessary to achieve selective and potent Cdc25 inhibition.

Discussion

Although there is consensus that DSPases have important roles in controlling cell proliferation and signaling pathways, the absence of potent and selective inhibitors has limited our ability to probe their biological function. For example, until recently the only readily available Cdc25 inhibitor was the broad spectrum PTPase inhibitor sodium orthovanadate. More recently, several small molecule Cdc25 phosphatase inhibitors have been reported such as dysidiolide (IC_{50} = 9.4 μM),[21] sulfircin (IC_{50} = 7.8 μM),[22] SC-ααδ9 (IC_{50} = 15 μM),[23] FY21-αα09 (IC_{50} = 7 μM),[24] a cyano-containing cholesteryl derivative (IC_{50} = 2.2 μM),[25] and a vitamin K analogue called **5** (IC_{50} = 3.8 μM).[26] Of interest to our study was the previous identification of tetrahydroisoquinolines with some inhibitory activity against Cdc25B (IC_{50} = 15–35 mM).[27] Most of the above-mentioned agents have not been evaluated for specificity and, with the exception of **5** and SC-ααδ9, none have been shown to inhibit Cdc25 within cells. Moreover, all of these compounds lack the desired potency for exceptional inhibitors.

Our studies illustrate how a subset of compounds selected from a chemical library based on chemical diversity can be used to screen against a predicted end point and yield potent bioactive compounds. The quinoline-5,8-diones have been the focus of previous studies because of their wide spectrum of biological activity including antitumor, antifungal, and antimalarial effects.[28] Despite considerable investigation, their mechanism of action is largely not understood. For quinolinediones, such as streptonigrin and lavendamycin, depletion of NADPH/NADH, uncoupling of oxidative phosphorylation, and/or DNA cleavage has been suggested.[29] Although we cannot formally exclude such mechanisms for the cytotoxic effects of NSC 663284, one advantage of our chemical complementation assay is that it provides one with the ability to examine cellular events after only a relatively brief exposure to an agent. This is especially important for agents that block cell proliferation. Thus, the chemical complementation assay provided experimental evidence that NSC 663284 can block the intracellular actions on the expressed target, namely, Cdc25A. Moreover, the regioisomer that was a superior inhibitor of Cdc25 in vitro was more cytotoxic after a brief cell exposure. Interestingly, we found no significant difference in the cytotoxicity of the two regioisomers when cells were treated continuously with these two regioisomers, suggesting that prolonged exposure may cause other toxic actions. Consistent with this notion is the observation that after prolonged exposure isoquinolinediones are more toxic to cells than their respective quinolinediones[30] even though in our studies the quinolinediones were more potent as in vitro inhibitors of Cdc25 than the corresponding isoquinolinediones (Table 2). Preliminary molecular modeling studies with the available crystal structures for Cdc25B are consistent with the quinolinedione pharmacophore binding in at least one of the Cdc25 anionic binding sites and provide a hypothetical explanation for the regioisomeric preference that can be tested with newer analogues (manuscript in preparation). As shown in the electrostatic potential maps, the nitrogen-substituted carbon of the ene-5,8-dione moiety in these inhibitors is the most electron-deficient center of the quinone substructure. While these computational electrostatic potential mapping studies suggest the need for an electron-deficient 7-position for maximal inhibitor activity, it is evident that the potency of inhibitors was not simply correlated with increasing electrophilicity at this position, which follows the series NSC 663284 < DA3003–2 < DA296 < DA3049. This would be consis-

tent with the notion that the pendant moieties on the 7-position also are important.

We noted some modest selectivity for inhibition of Cdc25A as compared with Cdc25B and Cdc25C. Although there is no available crystal structure of a ligand with any Cdc25 isoform, structural differences in the catalytic region of Cdc25A and Cdc25B have been noted.[16,17] Moreover, protein substrate preferences have been reported with Cdc25A and Cdc25C, which reflect not only residues within the catalytic domain but others as yet undefined outside of the catalytic domain.[17,18] Our results suggest that it may be feasible to identify small molecules with significant specificity for individual Cdc25 isoforms. These would be valuable reagents as there continues to be controversy about the precise cellular actions of some of the isoforms. We suggest that quinolinediones have a rich potential as a pharmacophore for inhibitors of the DSPase Cdc25 and that they could represent useful biochemical probes as well as possible lead compounds for the design of agents for the treatment of cancer or other diseases.[2,18]

Experimental Section

Library Chemicals. The Diversity Set and selected quinolinediones were the kind gift of Jill Johnson (NCI, National Institutes of Health, Developmental Therapetuics Program, Rockville, MD). The Diversity Set was generated by the NCI from the 140 000 compounds in the NCI Compound Repository based first on the availability of ≥1 g in their Repository, which reduced the total eligible compounds to 71 756. Chem-X (Oxford Molecular Group) was then used to define hydrogen bond acceptor, hydrogen bond donor, positive charge, aromatic, hydrophobic, acid, base, and distance intervals to create a particular finite set of pharmacophores. The default setting of 3-point pharmacophores resulted in almost 10^6 possible pharmacophores. The Chem-X diverse subset generating function was used to determine the acceptable conformations of individual structures and the acceptable pharmacophore for the conformation. The Diversity Set was populated in a comparative iterative manner with a requirement of ≤5 rotatable bonds. Because the selection procedure was order dependent, the order in which the structures were considered was randomized. This procedure resulted in the selection of 1990 compounds; more information about the NCI Diversity Set can be found at http://dtp.nci.nih.gov/.

Synthesis of Compounds. All moisture-sensitive reactions were performed under an atmosphere of dry nitrogen, and all glassware were dried in an oven prior to use. THF and ether were dried by distillation over sodium benzophenone and CH_2Cl_2 was dried by distillation over CaH_2. Unless otherwise stated, all commercially available materials were used without purification. IR spectra were recorded neat using NaCl cells. NMR spectra were obtained at 300 MHz/75 MHz ($^1H/^{13}C$ NMR) in $CDCl_3$ unless noted otherwise. High- and low-resolution masses were determined by introduction with a direct insertion probe into a VG-70-70 HF spectrometer operating in the electron ionization mode. The purity of synthetic DA3002, DA296, DA3003-1, DA3003-2, and DA3049 was ascertained by HRMS and HPLC analyses in two different mobile phases to be at least 94%, in most cases >99% (see Supporting Information for details of the analyses).

DA276 (Quinoline-5,8-dione). Prepared in 56% yield from quinoline-8-ol according to literature procedures:[31] ^1H NMR: δ 9.06 (dd, 1 H, J = 4.6, 1.6 Hz), 8.43 (dd, 1 H, J = 7.8, 1.6 Hz), 7.72 (dd, 1 H, J = 7.8, 4.6 Hz), 7.16 (d, 1 H, J = 10.0 Hz), 7.07(d, 1 H, J = 10.0 Hz). HRMS (EI) *m/z*: calcd for $C_9H_5NO_2$, 159.0320; found: 159.0321.

DA295 (6,7-Dichloroisoquinoline-5,8-dione). Prepared according to literature procedures:[30] ^1H NMR (MeOH-d_4, δ): 9.33 (s, 1 H), 9.08 (d, 1 H, J = 5.1 Hz), 8.08 (d, 1 H, J = 5.1 Hz). ^{13}C NMR (MeOH-d_4, δ): 173.8 (2C), 153.5, 146.7, 141.8, 141.7, 135.7, 123.4, 118.0. MS (EI) *m/z* (rel intensity): 227 (M^+, 100), 199 (20), 192 (80), 164 (80). HRMS (EI) *m/z*: calcd for $C_9H_3NO_2Cl_2$, 226.9541; found, 226.9544.

DA296 (6-Chloro-7-(2-morpholin-4-ylethylamino)isoquinoline-5,8-dione). A solution of DA295 (114 mg, 0.500 mmol) and 2-morpholin-4-ylethylamine (65 mg, 0.50 mmol) in 5 mL of THF was treated with triethylamine (0.07 mL, 0.5 mmol) at room temperature. The reaction mixture was stirred for 20 h at room temperature, concentrated under reduced pressure, diluted with ethyl acetate, and washed with water. The organic layer was dried (Na_2SO_4) and concentrated in vacuo. The crude residue was purified by chromatography on SiO_2 (CH_2Cl_2/MeOH, 15:1) to give a 4:1 mixture of DA296 and its regioisomer (110 mg, 69%). The major regioisomer was assigned based on ^1H NMR analysis.[32] Separation of isomers by chromatography on SiO_2 (CH_2Cl_2/MeOH, 50:1) or recrystallization from Et_2O/hexanes provided DA296 in ca. 90% purity as a dark red solid: mp 125 °C (dec). IR (neat): 3271, 2958, 2851, 1683, 1640, 1600, 1564, 1113 cm^{-1}. ^1H NMR: δ 9.24 (s, 1 H), 9.00 (d, 1 H, J = 5.0 Hz), 7.94 (d, 1 H, J = 5.0 Hz), 7.13 (br, 1 H), 4.02−3.96 (m, 2 H), 3.78−3.75 (m, 4 H), 2.69 (t, 2 H, J = 5.6 Hz), 2.54 (m, 4 H). ^{13}C NMR: δ 179.9, 175.0, 156.3, 154.3, 148.5, 138.2, 123.7, 119.1, 118.2, 67.0 (2C), 56.6, 53.0 (2C), 40.9. MS (EI) *m/z* (rel intensity): 323 ($[M + 2]^+$, 5), 221 (35), 101 (100). HRMS (EI) *m/z*: calcd for $C_{15}H_{18}N_3O_3Cl$ (M + 2H), 323.1037; found: 323.1037.

DA3002 (6,7-Dichloroquinoline-5,8-dione). Prepared in 30−40% yield from quinoline-8-ol according to literature procedures:[20] ^1H NMR (DMSO-d_6, δ): 9.01 (dd, 1 H, J = 3.8, 1.2 Hz), 8.41 (dd, 1 H, J = 7.3, 1.2 Hz), 7.86 (dd, 1 H, J = 7.3, 3.8 Hz). ^{13}C NMR (DMSO-d_6, δ): 176.0, 174.3, 154.5, 147.1, 143.1, 141.6, 134.9, 128.5, 128.3. MS (EI) *m/z* (relative intensity): 227 (M^+, 100), 199 (80), 192 (25), 136 (100). HRMS (EI) *m/z*: calcd for $C_9H_3NO_2Cl_2$, 226.9541; found: 226.9545.

DA3003-1 (NSC 663284, 6-Chloro-7-(2-morpholin-4-ylethylamino)quinoline-5,8-dione) and DA3003-2 (7-Chloro-6-(2-morpholin-4-ylethylamino)quinoline-5,8-dione). A solution of DA3002 (228 mg, 1.00 mmol) and 2-morpholin-4-ylethylamine (130 mg, 1.00 mmol) in 5 mL of THF was treated at room temperature with triethylamine (0.14 mL, 1.0 mmol). The reaction mixture was stirred for 20 h at room temperature, concentrated under reduced pressure, diluted with ethyl acetate, and washed with water. The organic layer was dried (Na_2SO_4) and concentrated in vacuo. The crude residue was purified by chromatography on SiO_2 (CH_2Cl_2/MeOH, 15:1) to give a 2:1 mixture (^1H NMR) of DA3003-1 and DA3003-2 (260 mg, 80%). Further separation by chromatography on SiO_2 (CH_2Cl_2/MeOH, 50:1) gave pure DA3003-1 and DA3003-2 as dark red, amorphous solids. The 5,8-quinolinedione regioisomers were assigned based on the known preference for nucleophilic addition at the 7-position in aprotic solvents and the observation that $\Delta\delta$ (H2−H4) of the 6-isomer is higher than that of the 7-isomer in ^1H NMR.[32] 5,8-Isoquinolinedione regioisomers were assigned based on the known preference for nucleophilic additions at the 7-position[33] and the apparent trend that $\Delta\delta$ (H1−H4) of the 6-isomer is higher than that of the 7-isomer in ^1H NMR.

DA3003-1. IR (neat): 3275, 2958, 2855, 1695, 1636, 1600, 1568, 1109 cm^{-1}. ^1H NMR: δ 8.92 (dd, 1 H, J = 4.7, 1.6 Hz), 8.48 (dd, 1 H, J = 7.8, 1.6 Hz), 7.66 (dd, 1 H, J = 7.8, 4.7 Hz), 7.09 (br, 1 H), 4.05−3.95 (m, 2 H), 3.80−3.70 (m, 4 H), 2.70 (t, 2 H, J = 5.7 Hz), 2.65−2.45 (m, 4 H). ^{13}C NMR: δ 179.0, 175.4, 153.4, 146.2, 145.3, 134.6, 129.8, 128.4, 67.0 (2C), 56.7, 53.0 (2C), 40.9. MS (EI) *m/z* (rel intensity): 323 ($[M + 2]^+$, 7), 210 (25), 100 (100). HRMS (EI) *m/z*: calcd for $C_{15}H_{18}N_3O_3Cl$ (M + 2H), 323.1037; found: 323.1034. A direct comparison between DA3003-1 and NSC 663284 showed no detectable difference in HPLC profiles, chemical properties, enzyme inhibitory effects, or growth inhibition. Thus, most of the reported cellular and kinetic studies were performed with NSC 663284 because of the limited amount of DA3003-1.

DA3003-2. IR (neat): 3275, 2958, 2851, 1687, 1647, 1600, 1564, 1106 cm^{-1}. ^1H NMR: δ 9.02 (dd, 1 H, J = 4.6, 1.6 Hz), 8.36 (dd, 1 H, J = 8.0, 1.6 Hz), 7.59 (dd, 1 H, J = 8.0, 4.6 Hz),

6.98 (br, 1 H), 4.0–3.9 (m, 2 H), 3.8–3.7 (m, 4 H), 2.70 (t, 2 H, $J = 5.4$ Hz), 2.6–2.45 (m, 4 H). ^{13}C NMR: δ 180.3, 175.2, 155.4, 148.6, 144.4, 134.8, 127.0, 126.7, 67.1 (2C), 56.8, 53.1 (2C), 40.8. MS (EI) *m/z* (rel intensity): 323 ([M + 2]$^+$, 40), 285 (8) 267 (10), 100 (100). HRMS (EI) *m/z*: calcd for $C_{15}H_{18}N_3O_3Cl$ (M + 2H), 323.1037; found: 323.1027.

DA3044 (6,7-Dichlorophthalazine-5,8-dione). Prepared according to literature procedures:[33] ^{1}H NMR: δ 9.93 (s, 2 H). MS (EI) *m/z* (rel intensity): 228 (M$^+$, 100), 200 (30). HRMS (EI) *m/z*: calcd for $C_8H_2N_2O_2Cl_2$, 227.9493; found: 227.9492.

DA3045 (6,7-Dichloroquinazoline-5,8-dione). Prepared according to literature procedures:[33] ^{1}H NMR: δ 9.75 (s, 1 H), 9.64 (s 1 H). MS (EI) *m/z* (rel intensity): 228 (M$^+$, 100), 200 (30), 165 (30), 110 (30), 87 (40). HRMS (EI) *m/z*: calcd for $C_8H_2N_2O_2Cl_2$, 227.9493; found: 227.9497.

DA3049 (6-Chloro-7-(2-morpholin-4-ylethylamino)phthalazine-5,8-dione). A solution of DA3044 (67 mg, 0.29 mmol) and 2-morpholin-4-ylethylamine (38 mg, 0.29 mmol) in 5 mL of THF was treated at room temperature with triethylamine (0.04 mL, 0.3 mmol). The reaction mixture was stirred for 2 h at room temperature, concentrated under reduced pressure, diluted with ethyl acetate, and washed with water. The organic layer was dried (Na_2SO_4) and concentrated in vacuo. The crude residue was purified by chromatography on SiO_2 (CH_2Cl_2/MeOH, 15:1) to give pure DA3049 (42 mg, 45%) as a dark red, amorphous sticky solid. IR (neat): 3271, 2958, 2923, 2855, 2808, 1695, 1636, 1556, 1311, 1295, 1113 cm^{-1}. ^{1}H NMR: δ 9.83 (s, 1 H), 9.65 (s, 1 H), 7.18 (br, 1 H), 4.00–3.90 (m, 2 H), 3.75–3.70 (m, 4 H), 2.69 (t, 2 H, $J = 6.0$ Hz), 2.55–2.50 (m, 4 H). ^{13}C NMR: δ 180.5, 174.2, 171.4, 147.2, 145.3, 144.5, 124.8, 123.3, 67.1 (2C), 56.3, 53.0 (2C), 41.0. MS (EI) *m/z* (rel intensity): 324 ([M + 2]$^+$, 10), 286 (12), 256 (8), 235 (12) 100 (100). HRMS (EI) *m/z*: calcd for $C_{14}H_{17}N_4O_3Cl$ (M + 2H), 324.0989; found: 324.0989.

DA3100 (6-Chloro-7-(indan-2-ylamino)quinoline-5,8-dione). According to the procedure described for DA3003-1, DA3100 (192 mg, 59%) was obtained from DA3002 (228 mg, 1.00 mmol) and 1-aminoindane (133 mg, 1.00 mmol) as a dark red, amorphous sticky solid. IR (neat): 3323, 3065, 2939, 2844, 1695, 1640, 1592, 1560, 1315, 721 cm^{-1}. ^{1}H NMR: δ 8.92 (dd, 1 H, $J = 4.6$, 1.4 Hz), 8.49 (dd, 1 H, $J = 7.8$, 1.4 Hz), 7.67 (dd, 1 H, $J = 7.8$, 4.6 Hz), 7.29–7.22 (m, 4 H), 6.40 (br, 1 H), 6.18–6.10 (m, 1 H), 3.13–2.92 (m, 2 H), 2.78–2.72 (m, 1 H), 2.13–2.06 (m, 1 H). ^{13}C NMR: δ 178.8, 175.8, 153.5, 146.0, 144.2, 143.5, 142.4, 134.8, 130.0, 128.8, 128.5, 127.3, 125.2, 124.5, 59.8, 36.3, 20.2. MS (EI) *m/z* (rel intensity): 324 (M$^+$, 30), 287 (15), 220 (15), 205(35), 117 (100). HRMS (EI) *m/z*: calcd for $C_{18}H_{13}N_2O_2Cl$, 324.0666; found: 324.0656.

In Vitro Enzyme Assays. The activities of the GST-fusion Cdc25A, Cdc25B$_2$, Cdc25C, and VHR as well as human recombinant PTP1B were measured using *o*-methyl fluorescein phosphate (Sigma, St. Louis, MO) as substrate and a miniaturized, 96-well microtiter plate assay based on previously described methods.[23] The final incubation mixtures (25 μL) were prepared using a Biomek 2000 laboratory automation workstation (Beckman Coulter, Inc., Fullerton, CA). Fluorescence emission from the product was measured after a 60-min incubation period at ambient temperature with a multiwell plate reader (PerSeptive Biosystems Cytofluor II; Framingham, MA; excitation filter, 485/20; emission filter, 530/30). Best curve fit for Lineweaver–Burk plots and K_i values were determined by using the curve-fitting programs Prism 3.0 (GraphPad Software, Inc., San Diego, CA) and SigmaPlot 2000 Enzyme Kinetics (SSPS Science, Richmond, CA).

Antiproliferative and Chemical Complementation Assays. The proliferation of human MCF-7 breast cancer cells was measured by a previously described colorimetric assay.[34] Briefly, we seeded 2000–4000 cells per well in microtiter plates and allowed them to attach overnight. Cells were then treated with vehicle or compound continuously or for 3 h. After a 48-h incubation in 5% CO_2 atmosphere and 100% humidity, the medium was replaced with serum-free medium containing 0.1% 3-(4,5-dimethylthiazol-2-yl)-2,5-diphenyltetrazolium bromide. Plates were incubated for an additional 3 h in the dark, and the total cell number was determined spectrophotometrically at 540 nm as previously described.[34]

For the chemical complementation assay, HeLa cells were obtained from ATCC and were maintained in Dulbecco's minimum essential medium (DMEM) containing 10% fetal bovine serum (FBS, HyClone, Logan, UT) and 1% penicillin–streptomycin (Life Technologies, Inc., Rockville, MD) in a humidified atmosphere of 5% CO_2 at 37 °C. We used a mammalian expression plasmid encoding full-length wild-type Cdc25A in a pcDNA3 vector generously provided by Thomas Roberts (Dana Farber Cancer Institute, Boston, MA)[3] as previously described.[20]

Acknowledgment. This work was supported by the U.S. Department of Defense, the Fiske Drug Discovery Fund, and the National Institutes of Health. We thank Daniel Zaharevitz and Jill Johnson of the NCI for providing compounds and advice.

Supporting Information Available: HPLC analysis results for DA compounds (with HRMS data). This material is available free of charge via the Internet http://pubs.acs.org.

References

(1) Denu, J. M.; Stuckey, J. A.; Saper, M. A.; Dixon, J. E. Form and function in protein dephosphorylation. *Cell* **1996**, *87*, 361–364.
(2) Nilsson, I.; Hoffmann, I. Cell cycle regulation by the Cdc25 phosphatase family. *Prog. Cell Cycle Res.* **2000**, *4*, 107–114.
(3) Xia, K.; Lee, R. S.; Narsimhan, R. P.; Mukhopadhyay, N. K.; Neel, B. G.; Roberts, T. M. Tyrosine phosphorylation of the proto-oncoprotein Raf-1 is regulated by Raf-1 itself and the phosphatase Cdc25A. *Mol. Cell. Biol.* **1999**, *19*, 4819–4824.
(4) Galaktionov, K.; Beach, D. CDC25 phosphatases as potential human oncogenes. *Cell* **1991**, *67*, 1181–1194.
(5) Sadhu, K.; Reed, S. I.; Richardson, H.; Russell, P. Human homolog of fission yeast Cdc25 mitotic inducer is predominantly expressed in G2. *Proc. Natl. Acad. Sci. U.S.A.* **1990**, *87*, 5139–5143.
(6) Nagata, A.; Igarashi, M.; Jinno, S.; Suto, K.; Okayama, H. An additional homolog of the fission yeast cdc25+ gene occurs in humans and is highly expressed in some cancer cells. *New Biol.* **1991**, *3*, 959–968.
(7) Galaktionov, K.; Lee, A. K.; Eckstein, J.; Draetta, G.; Meckler, J.; Loda, M.; Beach, D. CDC25 phosphatases as potential human oncogenes. *Science* **1995**, *269*, 1575–1577.
(8) Galaktionov, K.; Chen, X.; Beach, D. Cdc25 cell-cycle phosphatase as a target of c-myc. *Nature* **1996**, *382*, 511–517.
(9) Wu, W.; Fan, Y.-H.; Kemp, B. L.; Walsh, G.; Mao, L. Overexpression of *cdc*25A and *cdc*25B is frequent in primary non-small cell lung cancer but is not associated with overexpression of c-*myc*. *Cancer Res.* **1998**, *58*, 4082–4085.
(10) Giulia Cangi, M.; Cukor, B.; Soung, P.; Signoretti, S.; Moreira, J., G.; Ranashinge, M.; Cady, B.; Pagano, M.; Loda, M. Role of the Cdc25A phosphatase in human breast cancer. *J. Clin. Invest.* **2000**, *106*, 753–761.
(11) Millar, J. B.; Blevitt, J.; Gerace, L.; Sadhu, K.; Featherstone, C.; Russell, P. p55CDC25 is a nuclear protein required for the initiation of mitosis in human cells. *Proc. Natl. Acad. Sci. U.S.A.* **1991**, *88*, 10500–10504.
(12) Hoffman, I.; Draetta, G.; Karsenti, E. Activation of the phosphatase activity of human cdc25A by a cdk2-cyclin E dependent phosphorylation at the G1/S transition. *EMBO J.* **1994**, *13*, 4302–4310.
(13) Jinno, S.; Suto, J.; Nagata, A.; Igarashi, M.; Kanaoka, Y.; Nojima, H.; Okayama, H. Cdc25A is a novel phosphatase functioning early in the cell cycle. *EMBO J.* **1994**, *13*, 1549–1556.
(14) Molinari, M.; Mercurilo, C.; Dominguez, J.; Goubin, F.; Draetta, G. F. Human Cdc25 A inactivation is response to S phase inhibition and its role in preventing premature mitosis. *EMBO Rep.* **2000**, *1*, 71–79.
(15) Mailand, N.; Falck, J.; Lukas, C.; Syljuasen, R. G.; Welcker, M.; Lukas, J. Rapid destruction of human Cdc25A in response to DNA damage. *Science* **2000**, *288*, 1425–1429.
(16) Fauman, E. B.; Cogswell, J. P.; Lovejoy, B.; Rocque, W. J.; Holmes, W.; Montana, V. G.; Piwnica-Worms, H.; Rink, M. J.; Saper, M. A. Crystal structure of the catalytic domain of the human cell cycle control phosphatase, Cdc25A. *Cell* **1998**, *93*, 617–625.
(17) Reynolds, R. A.; Yem, A. W.; Wolfe, C. L.; Deibel, J. M. R.; Chidester, C. G.; Watenpaugh, K. D. Crystal structure of the catalytic subunit of Cdc25B required for G2.M phase transition of the cell cycle. *J. Mol. Biol.* **1999**, *293*, 559–568.

(18) Rudolph, J.; Epstein, D. M.; Parker, L.; Eckstein, J. Specificity of natural and artificial substrates for human Cdc25A. *Anal. Biochem.* **2001**, *289*, 43−51.
(19) Chen, W.; Wilborn, M.; Rudolph, J. Dual-specific Cdc25B phosphatase in search of the catalytic acid. *Biochemistry* **2000**, *39*, 10781−10789.
(20) Vogt, A.; Adachi, T.; Ducruet, A. P.; Chesebrough, J.; Nemoto, K.; Carr, B. I.; Lazo, J. S. Spatial analysis of key signaling proteins by high-content solid-phase cytometry in Hep3B cells treated with an inhibitor of Cdc25 dual specificity phosphatases. *J. Biol. Chem.* **2001**, *276*, 20544−20550.
(21) Gunasekera, S. P.; McCarthy, P. J.; Kelly-Borges, M. Dysidiolide: A novel protein phosphatase inhibitor from the Caribbean sponse dysidea etheria de laubenfels. *J. Am. Chem. Soc.* **1996**, *118*, 8759−8760.
(22) Cebula, R. E.; Blanchard, J. L.; Boisclair, M. D.; Pal, K.; Bockovich, N. J. Synthesis and phosphatase inhibitory activity of analogs of sulfircin. *Bioorg. Med. Chem. Lett.* **1997**, *7*, 2015−2020.
(23) Rice, R. L.; Rusnak, J. M.; Yokokawa, F.; Yokokawa, S.; Messner, D. J.; Boynton, A. L.; Wipf, P.; Lazo, J. S. A targeted library of small molecule, tyrosine and dual specificity phosphatase inhibitors derived from a rational core design and random side chain variation. *Biochemistry* **1997**, *36*, 15965−15974.
(24) Ducruet, A. P.; Rice, R. L.; Tamura, K.; Yokokawa, F.; Yokokawa, S.; Wipf, P.; Lazo, J. S. Identification of new Cdc25 dual specificity phosphatase inhibitors in a targeted small molecule array. *Bioorg. Med. Chem.* **2000**, *8*, 1451−1466.
(25) Peng, H.; Xie, W.; Otterness, D. M.; Cogswell, J. P.; McConnell, R. T.; Carter, H. L.; Powis, G.; Abraham, R. T.; Zalkow, L. H. Synthesis and biological activities of a novel group of steroidal derived inhibitors for human Cdc25A protein phosphatase. *J. Med. Chem.* **2001**, *44*, 834−848.
(26) Tamura, K.; Southwick, E. C.; Kerns, J.; Rosi, K.; Carr, B. I.; Wilcox, C.; Lazo, J. S. Cdc25 inhibition and cell cycle arrest by a synthetic thioalkyl vitamin K analogue. *Cancer Res.* **2000**, *60*, 1317−1325.
(27) Fritzen, E. L.; Brightwell, A. S.; Erickson, L. A.; Romero, D. L. The solid phase synthesis of tetrahydroisoquinolines having Cdc25B inhibitory activity. *Bioorg. Med. Chem. Lett.* **2000**, 649−652.
(28) Behforouz, M.; Haddad, J.; Cai, W.; Gu, Z. Chemistry of quinoline-5,8-diones. *J. Org. Chem.* **1998**, 63, 343−346.
(29) Boger, D. L.; Yasuda, M.; Mitscher, L. A.; Drake, S. D.; Kitos, P. A.; Thompson, S. C. Streptonigrin and lavendamycin partial structures. Probes for the minimal, potent pharmacophore of streptonigrin, lavendamycin, and synthetic quinoline-5,8-diones. *J. Med. Chem.* **1987**, *30*, 1918−1928.
(30) Ryu, C.-K.; Lee, I.-K.; Jung, S.-H.; Lee, C.-O. Synthesis and cytotoxicity of 6-chloro-7-arylamino-5,8-isoquinolinediones. *Bioorg. Med. Chem. Lett.* **1999**, *9*, 1075−1080.
(31) Cameron, D. W.; Deutscher, K. R.; Feutrill, G. I. Nucleophilic alkenes. IX. Addition of 1,1-dimethoxyethene to azanaphthoquinones: Synthesis of bostrycoidin and 8-*O*-methylbostrycoidin. *Aust. J. Chem.* **1982**, *35*, 1439−1450.
(32) Yoon, E. Y.; Choi, H. Y.; Shin, K. J.; Yoo, K. H.; Chi, D. Y.; Kim, D. J. The regioselectivity in the reaction of 6,7-dihaloquinoline-5,8-diones with amine nucleophiles in various solvents. *Tetrahedron Lett.* **2000**, *41*, 7475−7480.
(33) Shaikh, I. A.; Johnson, F.; Grollman, A. P. Streptonigrin. 1. Structure−activity relationships among simple bicyclic analogues. Rate dependence of DNA degradation on quinone reduction potential. *J. Med. Chem.* **1986**, *29*, 1329−1340.
(34) Vogt, A.; Rice, R. L.; Settineri, C. E.; Yokokawa, F.; Yokokawa, S.; Wipf, P.; Lazo, J. S. Disruption of insulin-like growth factor-1 signaling and down-regulation of Cdc2 by SC-ααδ9, a novel small molecule antisignaling agent identified in a targeted array library. *J. Pharmacol. Exp. Therap.* **1998**, *287*, 806−813.

JM0102046

J Exp Ther Oncol

In press

Local Administration of IL-12-transfected Dendritic Cells Induces Antitumor Immune Responses to Colon Adenocarcinoma in the Liver in Mice

Yuji Satoh[*§], Clemens Esche[*#], Andrea Gambotto[*†θ], Galina V. Shurin[*#], Zoya R. Yurkovetsky[θ], Paul D. Robbins[θ], Simon C. Watkins[‡], Satoru Todo[§], Michael T. Lotze[*†1], Ronald B. Herberman[*#], Michael R. Shurin[*#]

[*]Biologic Therapeutics Program, University of Pittsburgh Cancer Institute
Departments of [#]Pathology, [†] Surgery, and [θ]Biochemistry and Molecular Genetics
[‡] Center for Biologic Imaging
University of Pittsburgh School of Medicine, Pittsburgh, PA 15261, USA
and
[§] First Department of Surgery, Hokkaido University School of Medicine, Sapporo, Japan

Running Title: Immune gene therapy of liver metastases

Key Words: Dendritic cells, IL-12, Immunotherapy, Liver tumor

Correspondence:

Michael R. Shurin, MD, PhD
University of Pittsburgh Cancer Institute
Clinical Immunopathology
5725 CHP-MT
200 Lothrop Street
Pittsburgh, PA 15213
Phone: 412-647-6140

ABSTRACT

Colorectal cancer is one of the most common fatal malignancies in the United States, with an incidence second only to lung cancer. The liver is the most common site of colorectal metastases and frequently the only affected organ once the primary tumor has been surgically removed. The only potentially curative treatment for metastatic colorectal cancer in the liver is surgery, although most patients are not eligible for resection. We have therefore evaluated the therapeutic efficacy of dendritic cells (DC) engineered to express IL-12 in a liver metastasis model. Direct administration of DC into the portal vein significantly inhibited the growth of established MC38 colon carcinoma in the liver in C57BL/6 mice. This effect was accompanied by an intratumoral accumulation of CD4+, CD8+, and NLDC-145+ immune effector cells, and also resulted in a systemic immune response as determined by enhanced production of IFN-γ by T lymphocytes isolated from both spleen and draining lymph nodes. Evaluation of homing of Cy3-labeled DC following the portal vein injection confirmed their distribution in the liver and lymphoid tissue. Thus, a local delivery of DC transduced with the IL-12 gene can not only inhibit colorectal tumor growth *in vivo* but also mount systemic antitumor immune responses. This approach is likely to improve the outcome of immunotherapy for metastatic colorectal cancer since high numbers of tumor-associated DC positively correlate with a more favorable prognosis. Simultaneous local gene therapy with IL-12 will further improve clinical efficacy without placing the patient at risk for systemic toxicity.

INTRODUCTION

Colorectal cancer is one of the most common fatal malignancies in the United States, with an incidence second only to lung cancer. Approximately 135,400 new cases and more than 56,700 deaths due to colorectal cancer are expected for 2001 (Greenlee et al., 2001). In spite of extensive efforts over the last decades, only modest improvements in overall survival of patients with colorectal cancer have been accomplished through refinements of surgery, chemotherapy and radiotherapy (Chen et al., 2000). Nonetheless, 50% of affected patients will develop recurrent or metastatic disease and most will die as a consequence (Chen et al., 2000). The liver is the most common site of colorectal metastases and frequently the only affected organ (Fong, 1999). When untreated, such metastases are uniformly fatal with a median survival of about two months and the only potentially curative treatment for metastatic colorectal cancer in the liver is surgery (Fong, 1999). However, most patients with colorectal liver metastases are not eligible for resection because of either multiple lesions or anatomical constraints (Hewitt et al., 1998). Therefore, new therapeutic approaches need to be developed. A promising experimental strategy for colorectal cancer is immunotherapy, which is expected to provide a more tumor-specific activity, thereby being less toxic to normal cells than standard modalities. In fact, Immunologic approaches for colorectal cancer therapy have already evolved substantially (Foon, 2001).

The generation of an antitumor immune response involves the interaction of several cell types. The ability to present antigens to naïve T cells represents the most crucial function of dendritic cells (DC), antigen-presenting cells (APC) with a unique ability to induce primary immune responses (Steinman, 2001). DC generated with *ex vivo* GM-CSF and IL-4 require further stimulation in order to fully develop their capability to present tumor-associated antigens and thereby to generate tumor specific immunity (Esche et al., 1999b). Bacterial products, such as LPS, and cytokines including IL-1, TNF-α and CD154 can induce DC activation, resulting in a switch of DC function from antigen uptake (functionally "immature" or "non-activated" DC) to antigen presentation (functionally "mature" or "activated" DC). This process is accompanied by the induction of IL-12 synthesis (Koch et al., 1996), an absolute requirement for initiation of cellular antitumor immune responses. We therefore hypothesized that DC genetically modified to express IL-12 will represent a powerful immunotherapeutic approach for metastatic colorectal cancer. However, the most appropriate route of DC delivery remains to be established.

The DC growth factor Flt3 ligand is capable of mobilizing DC into the peripheral blood of patients with metastatic colon cancer and may be associated with increases in DC infiltration in the peritumoral regions (Morse et al., 2000). This approach is likely to improve the outcome of immunotherapy for colorectal cancer since high numbers of tumor-associated DC (TADC) directly correlate with a more favorable prognosis (Schwaab et al., 2001; Shurin and Gabrilovich, 2001). However, we have reported that both murine and human DC undergo premature apoptotic death in the tumor microenvironment (Esche et al., 1999a; Shurin et al., 1999a), suggesting that additional treatment of DC is required to protect them from tumor-induced apoptosis. IL-12, a cytokine with a strong antitumor activity, has been shown to induce DC generation, prolong their survival, and increase DC resistance to tumor-induced cell death (Esche et al., 2000a; Pirtskhalaishvili et al., 2000a; Shurin et al., 1997a). On the other hand, only locoregional application of DC guarantees their highest accumulation at the tumor site and minimizes IL-12-related toxicity (Esche et al., 2000b; Shurin et al., 2000). Indeed, it has been recently demonstrated that peritumoral injection of IL-12-transduced DC is capable of inhibiting the growth of CT26 colon carcinoma or prostate carcinoma using a subcutaneous model in mice (Furumoto et al., 2000; Pirtskhalaishvili et al., 2000b). Since only a metastases model can simulate the specific biology of liver metastases

(Radinsky and Ellis, 1996), we have evaluated a direct injection of MC38 tumor cells into the liver prior to using the portal vein for therapeutic administration of genetically modified DC.

In this study, we have demonstrated that a direct portal administration of IL-12-transfected DC represents a feasible and effective approach of treating established metastatic colorectal adenocarcinoma in the liver. This strategy not only inhibited tumor growth but also resulted in induction of Th1-biased systemic immune responses suggesting that local delivery of IL-12-producing DC represents a promising modality for immunotherapy of liver metastases not only in inoperable patients but also in an adjuvant setting.

MATERIAL AND METHODS

Cell culture, reagents and cytokines. MC38 colon carcinoma cells (kindly provided by Dr. Steven Rosenberg, NCI) and MF57B$^-$ fibroblasts (kindly provided by Dr. Timothy Carlos, UPCI) were maintained in RPMI medium supplemented with 5% fetal bovine serum, 100 units/100 μg/ml penicillin/streptomycin, 1 mM sodium pyruvate, 2 mM L-glutamine, and 0.1 mM non-essential amino acids at 37°C in 5% CO_2. Tissue culture reagents were obtained from Sigma Chemical Co. (St. Louis, MO) or Life Technologies Inc. (Grand Island, NY). Murine recombinant GM-CSF and IL-4 were purchased from R&D Systems Inc. (Minneapolis, MN).

Mice and a tumor model. Male C57BL/6 mice (6-8 weeks old) were obtained from Taconic (Germantown, NY) and housed in transparent plastic cages under pathogen-free conditions, 4-5 mice per cage, controlled temperature and humidity, a 12-h light:dark cycle with sterile food, and water *ad libitum*. Mice were acclimatized for at least two weeks prior to experimentation.

For tumor cell injection, animals were anesthetized in a methoxyflurane (Pitman-Moor, Mundelein, IL) chamber and the abdomen was opened via a midline skin incision. Using a 30-gauge needle, 1 ml disposable syringe, and a calibrated push button-controlled dispensing device (Hamilton Syringe Company, Reno, NV), 50 μl of a MC38 tumor cell suspension (5×10^5 cells/mouse) were injected under the capsule of the left medial liver lobe. To prevent leakage, a cotton swab was held over the injection site for 2 min. Skin and peritoneum were closed in a single layer using a nylon suture. The procedure was well tolerated by all animals and no intra-operative or anesthesia-related deaths occurred. Mice were randomized to one of six groups (4-5 mice/group), with no statistically significant difference between the mean body weights of the groups. Tumor size was determine on harvested levers by determination of tumor length in two perpendicular directions and expressed as tumor areas in mm^2. The University of Pittsburgh Animal Care Committee reviewed and approved all procedures.

Dendritic cell generation. The generation of murine bone marrow-derived DC in cultures was performed as described earlier (Esche et al., 1999a). Briefly, murine femur and tibia marrow cell suspensions were passed through a 70 μm nylon mesh and depleted of erythrocytes using 155 mM NH_4Cl in 10 mM Tris-HCl buffer (pH 7.5). T and B cells were depleted using a mixture of anti-CD4, anti-CD8 and anti-B220 monoclonal antibodies (hybridoma supernatants obtained from RL-172, TIB-105 and TIB-146 cell lines, respectively; ATCC, Rockville, MD) and Low-Tox-M rabbit complement (Cedarline Lab., San Diego, CA). To remove macrophages, cells were placed in 6-well plates (Falcon, Lincoln Park, NJ) at a concentration of 10^6 cells/ml in a complete medium (RPMI 1640, 10% heat-inactivated FCS, 10 mM Hepes, 0.1 mM non-essential amino acids, 1 mM sodium pyruvate, 2 mM glutamine, 50 μg/ml gentamicin sulfate, 1 μg/ml indomethacin, 50 μM N^G-nitro-L-arginine methyl ester) at 37°C. After an overnight incubation, non-adherent and loosely adherent cells were replated at 2 x 10^5 cells/ml in a complete medium supplemented with 1000 U/ml *rm*GM-

CSF and *rm*IL-4. At Day 4, half of the medium in each well was removed and replaced with an equivalent volume of cytokine-supplemented medium.

To determine DC phenotype, DC were washed in FACS medium (HBSS containing 0.1 % BSA and 0.1 % NaN_3) and stained with appropriately diluted antibodies directly conjugated with FITC or PE at 4 °C for 30 min. For the non-conjugated antibodies, corresponding secondary antibodies were used after blocking procedures. All antibodies were from Serotec (Washington, DC) or PharMingen (San Diego, CA). After fixation in 1% paraformaldehyde, samples were analyzed using FACScan (Becton Dickinson, Franklin Lakes, NJ) and LYSYS II software. Cultured DC expressed high levels of CD11c, CD80, CD86, CD40, and MHC class I molecules and the viability of cells was greater than 95%.

To evaluate functional activity of DC, their ability to induce proliferation of allogeneic T cells was assessed in the MLR assay as described (Shurin et al., 1997b). Briefly, allogeneic T cells (H-$2K^d$) were isolated from the spleens by a nylon-wool based filtration and plated in triplicates in 96-well round bottom plates ($3x10^5$cells/well, 100 µl). DC (H-$2K^b$) were added in different ratios (100 µl) and mixed cultures were incubated for 96 h at 37°C. Cell cultures were pulsed with 1µCi/well ^{3}H-thymidine (5 Ci/mmol; DuPont-NEN, Boston, MA) during the last 16-18 h and harvested on to GF/C glass fiber filter paper (Whatman Intl. Ltd, Maidstone, England) using a MACH III microwell harvester (Tomtec, Hamden, CT). Incorporation of ^{3}H-thymidine was determined on a MicroBeta TRILUX liquid scintillation counter (WALLAC, Gaithersburg, MD). The counts were expressed as a count per minute (cpm).

Adenoviral vector. Construction and characterization of the adenovector (type 5, E1/E3 deleted) expressing *m*IL-12 have been described previously (Gambotto et al., 1999). In brief, pAdCMV-*m*IL-12 was constructed by transferring a *Bgl*II/*Bam*HI fragment containing the p40 subunit of *m*IL-12 into the *Bam*HI site of pAdCMV-B. A *Bam*HI fragment containing the p35-encoding gene was subsequently cloned in the *Bam*HI site behind the p40 subunit. This resulted in a polycistronic message expressing both subunits of *m*IL-12. Virus generated by recombination between the shuttle vector and the Ad DNA was propagated on 293 cells and purified from infected cells 2 days after infection by three freeze-thaw cycles followed by three successive bandings on CsCl gradients.

Dendritic cell transfection and injection. Non-adherent cells (10^6) from a Day 5 DC culture were infected with adenovirus supernatant (50 µl) at a multiplicity of infection (MOI) of 100 for 1 h in 0.5 ml of serum-free medium in 24-well plates at 37°C. Next, 1 ml of fresh medium supplemented with GM-CSF, IL-4 and 20% FCS was added and DC were incubated for the additional 48 h. Transfected cells were washed in PBS and the transfection efficiency was measured analyzing a GFP expression by the FACScan (Becton Dickinson, Mountain View, CA) or epifluorescence microscope (Nikon). The viability of DC after transfection was > 70% and all dead cells were isolated by a gradient centrifugation.

Murine fibroblasts, served as a control, were transduced using the identical procedures.

For administration of DC, mice were anesthetized using methoxyflurane prior to laparotomy and exposure of the portal vein was performed through a small midline incision. Control non-transfected DC, GFP-transfected DC, IL-12-transfected DC, control fibroblasts or IL-12-transfected fibroblasts (1 x 10^6 cells/mouse) were injected intraportally using a 27-gauge needle at Day 7 after inoculation of tumor cells under the liver capsule. Tumor areas in liver on Day 7 ranged from 4 to 9 mm^2 (6.5 ± 2.5 mm^2, n= 9), as was determined in the preliminary studies. All experiments were repeated twice and the mean data from 3 independent experiments are presented. Animals were sacrificed by a cervical dislocation on Day 21. The sizes of the tumors in the livers were measured

by a caliper. Spleen, tumor, para-aortal and hepatic lymph nodes were collected and small pieces of tissue were frozen in O.C.T. compound and stored at -80°C for the immunohistochemical analysis. In addition, splenic and lymph node T cells were harvested for further determination of their activity.

Immunohistochemistry. Six μm cryostat sections of tumor samples were air-dried overnight and fixed in acetone. Non-specific staining was blocked using the SP-2001 avidin/biotin kit (Vector Laboratories, Inc., Burlingame, CA). Slides were washed with PBS, and incubated for 1 h at room temperature with the appropriate dilutions of NLDC-145 (Serotec, Washington, D.C.), anti-CD4, or anti-CD8 antibodies (PharMingen). A 1:500 dilution of biotinylated mouse anti-rat IgG (Jackson ImmunoResearch Laboratories, West Grove, PA) was applied as the secondary antibody for 45 min. The color reaction was developed for 8 min using the peroxidase chromogen kit (AEC, Biomega Corp., Foster City, CA). Sections were counterstained with hematoxylin. Negative controls included staining with the corresponding isotype for each antibody and staining with secondary antibody alone. Positive controls included immunostaining of known positive tissues. All results were obtained from a minimum of two independent specimens in each experiment. Two experienced investigators read the slides blindly and determined the number of positive cells/tissue section by analyzing at least 20 different areas.

Dendritic cell migration *in vivo*. Fluorescent microscopy was performed using a Nicon microscope and the images were captured using a cooled charge coupled device camera (Photometrics, Tucson, AZ) and SmartCapture software (Digital Scientific, Cambridge, United Kingdom). Images were further processed using Adobe Photoshop software (Adobe Systems, Mountain View, CA). Cultured DC were labeled with Cy3, a water-soluble cyanine dye (1 μg/ml, 37°C, 30 min), washed, and injected into the portal vein of tumor-bearing mice as described above. As a control, labeled DC were also injected in the vena cava. Four, 24 and 48 h later, tumor tissue, liver, and spleen were collected, frozen, sliced and analyzed immediately. Labeled DC were detected with TRITC filter sets.

Cytokine production. T cells isolated from spleens or lymph nodes and enriched on nylon wool columns were stimulated with irradiated (10,000 rad) MC38 tumor cells or irrelevant B16 melanoma cells. Supernatants were collected 0-72 hrs later, centrifuged (2000 g, 15 min) and stored at -20°C. Concentrations of *m*IFN-γ protein were determined using a commercial ELISA kit (Genzyme, Cambridge, MA) and expressed as pg/10^6 cells/36 h. Concentrations were calculated using recombinant cytokines as standards.

IL-12 production by control and transfected DC or fibroblasts was detected in cell-free supernatant using p70 IL-12 ELISA kit (R&D System, Minneapolis, MN).

Data analysis. Statistical significance of differences between the mean tumor sizes and cytokine production in different groups were analyzed using a one-way ANOVA after evaluation for normality. All pairwise multiple comparison procedures used the Student-Newman-Keuls method. For a single comparison of two groups, the Student *t*-test was applied. The level of significance was set at a probability of 0.05. Data are presented as the mean ± SE of the mean.

RESULTS

Adenoviral transfection of DC with mIL-12 gene

We have first demonstrated the high levels of protein expression after transduction with adenoviral vector encoded murine IL-12 gene in both DC and fibroblasts. As shown in Fig.1, both cultured DC and fibroblast cell line produced high levels of IL-12 after genetic modification with IL-12 gene. In contrast to non-transfected cells, no additional stimulation of DC was required to release IL-12 protein. Interestingly, IL-12 transfected fibroblasts expressed slightly higher levels of IL-12 when compared with IL-12-transfected DC (Fig.1). For instance, IL-12-transfected DC produced 18.61 ± 2.94 ng/10^6cells/96h of IL-12 while fibroblasts transduced with IL-12 gene produced 24.64 ± 0.27 ng/10^6cells/96h of IL-12. Non-transfected DC or fibroblasts, as well as GFP-transfected DC produce <3 pg/ml of IL-12 without additional stimulation with bacterial products or CD40 ligand. Thus, these data suggest that AdenoIL-12 vector transfects both DC and fibroblasts with a high efficiency.

Efficiency of adenovector-based transfection of DC was determined by analysis of expression of GFP on GFP-transduced DC. The average range of transfection efficiency was between 70-90 %, as determined by FACScan analysis. These results were confirmed by the fluorescent microscopy of GFP-transfected DC cultures (data not shown).

In addition, we have demonstrated that IL-12-transduced DC express higher levels of MHC class I, CD86, CD80, and CD40 molecules in comparison with non-transfected or control-transfected DC. To control the transfection procedure, DC were transduced with a LacZ gene instead of GFP gene in order to determine the expression of cell surface molecules by a FACScan (Fig.2). For instance, the percentage of double-positive CD11c+ DC co-expressing CD80, CD86, and CD40 increased up to 133%, 215%, and 268%, respectively, in DC cultures transfected with IL-12 gene in comparison with non-transfected DC ($p<0.0001$). Although LacZ-transfected DC expressed slightly higher levels of CD80, CD86 and CD40 molecules than non-transfected DC, this increase was significantly lower when compared with IL-12-transfected cells ($p<0.0001$). Thus, these data demonstrate that IL-12-transfected DC express significantly higher levels of cell surface molecules, which play a crucial role in DC/T cell interaction. They also suggest that genetically modified DC might be stronger inducers of T cell activation and proliferation. To test this hypothesis, the stimulatory potential of transfected and control DC was examined in an allogeneic MLR assay. Analysis of the results of these experiments revealed that IL-12-transfected DC caused significantly higher levels of T lymphocyte proliferation when compared with non-transfected or control protein-transfected DC: 51,816±2,266 cpm, 35,886±9,887 cpm, and 27,799±4,052 cpm for IL-12-transfected, LacZ-transfected, and non-transfected DC, respectively (optimal DC/T cell ratio 1:20; $p<0.01$).

Together these *in vitro* data demonstrate that adenoviral transduction of DC with IL-12 gene results in a higher level of protein expression accompanied by DC activation and increased ability to stimulate T cells. They also justify the evaluation of antitumor properties of transfected DC in *in vivo* experiments.

Local administration of IL-12-transfected DC into the portal vein inhibited growth of MC38 colon adenocarcinoma in the liver

Next, we have determined whether a local administration of control or genetically engineered cells induce antitumor immunity and inhibit tumor growth in a murine model of colon cancer metastasis in the liver. Fig. 3 summarizes the MC38 tumor growth data from three independent experiments and demonstrates that the vaccination of tumor-bearing animals with IL-12-transfected DC resulted in a significant growth inhibition of the established liver tumors as compared with the control vaccination containing non-transfected or GFP-transfected DC: 174.5 ± 17.6 mm^2 vs 503.6 ± 30.5 mm^2 and 490.3 ± 55.5 mm^2, respectively ($p<0.0001$). The average area of non-treated liver tumors

was 673.0 ± 84.2 mm^2. Thus, IL-12 transfection appears to represent a significant improvement regarding the therapeutic outcome of locally administered DC vaccinations. Interestingly, IL-12 transfected fibroblasts administered into the portal vein also displayed a significant inhibition of tumor growth when compared with non-treated animals: 349.6 ± 17.7 mm^2 ($p<0.05$), representing an antitumor effect of locally produced IL-12. As expected, IL-12-transfected fibroblasts were significantly less efficient in inhibition of tumor growth than IL-12-transfected DC ($p<0.0001$), while non-transfected fibroblasts did not produce any significant antitumor effect in our tumor model (815.3 ± 40.6 mm^2, $p=0.29$). Although non-transduced DC and GFP-transduced DC performed a slight inhibition of tumor growth (Fig.3), these effects were not significant in comparison with the non-treated group of mice ($p=0.11$ and 0.09, respectively). Thus, the transfection-induced potentiation of the observed antitumor effect is the direct result of a synergy between IL-12 and DC and cannot be achieved by using a different carrier cell. Importantly, daily monitoring of all mice did not reveal any evidence for systemic toxicity.

Intraportal administration of labeled DC resulted in a short-term homing of labeled DC in the liver, spleen, and liver metastasis

To determine trafficking and homing of DC following the intraportal administration, we have labeled DC with Cy3 fluorochrom dye and analyze their presence in lymphoid and non-lymphoid tissues at different times after injection. The data from two independent experiments are presented in Table I. As can be seen, intraportal administration of DC resulted in a temporal homing of cells within the liver and spleen during the first 24 h after injection. A smaller accumulation of labeled DC was also detected in the draining lymph nodes 24 h after DC administration. Interestingly, only a few labeled DC were determined within the tumor tissue (Table I). Control injection of Cy3-labeled DC into the vena cava resulted in higher levels of DC trafficking to the lymphoid tissue in comparison to the liver, and no homing within the tumor mass. Fig.4 demonstrates localization of injected DC in the liver, spleen and tumor at different time-points after injection. Unexpectedly, almost no labeled cells were detected at the site of the tumor at early and late time-points, suggesting different mechanisms of DC homing within the tumor-free liver tissue and liver metastasis.

DC-induced inhibition of tumor growth was associated with accumulation of CD4+, CD8+, and NLDC-145+ cells at the metastasis site

Since the increased infiltration of colon cancer tissue with the immune cells is associated with a prolonged patient survival (Schwaab et al., 2001), we next evaluated the amount of both T cells and DC within the liver metastases obtained from treated and control animals. Table II summarizes the results of immunohistochemical determination of tumor infiltrating T cells and DC. As expected, only immunotherapy with IL-12-transfected DC resulted in a significantly higher infiltration of tumor tissue with both CD4+ and CD8+ T lymphocytes, as well as DC. Spleens collected from treated and control animals did not display any significant alterations in T cells and DC content with the only exception of increased numbers of CD4+ T cells in animals treated with IL-12-transfected DC. Fig.5 shows tumor infiltration by T cells and DC two weeks after administration of IL-12-transfected (left panels) or GFP-transfected (right panels) DC injected into the portal vein. A significantly higher level of tumor infiltration by CD4+, CD8+ T cells and NLDC145+ DC can be observed. No significant differences in T and DC infiltration of the tumor mass between groups treated with GFP-transfected DC and other tested cellular vaccines were observed. Together, these data demonstrate that local administration of IL-12-producing DC results in a prolong stimulation of

antitumor immune response associated with a local accumulation of immune effectors at the tumor site and inhibition of tumor growth.

Intraportal therapy with IL-12-transfected DC induced a systemic antitumor immune response

To evaluate whether the local administration of IL-12-transfected DC elicits a systemic immune response, we have next determined the plasma levels of IL-12 and IFN-γ in dynamics after injection of different DC-based vaccines (Table III). As expected, administration of IL-12-transduced DC caused a marked elevation of systemic levels of both IL-12 and IFN-γ peaked at 24-48 h after injection ($p<0.001$). No alterations of IL-4 concentrations were observed at any time points. Non-transfected and GFP-transfected DC had no effect on tested cytokines after intraportal administration. These findings thus suggest that IL-12-transfected DC might non-specifically boost systemic immunity at early time-points after vaccination.

Next, to test whether DC-based vaccination of liver tumor-bearing mice results in the development of specific systemic antitumor immune responses, both lymph node and splenic T cells obtained from treated and non-treated mice were stimulated with irradiated relevant (MC38) or irrelevant (EL4) tumor cells *in vitro*. The maximum increased production of IFN-γ upon stimulation with MC38, which reflects the presence of tumor-specific T cells, was observed in T cell cultures obtained from animals treated with IL-12-transfected DC ($p<0.0001$). For instance, stimulated lymph node T cells released 24,434±202, 288±21, and 244+11 pg/ml/10^6cells/36h of IFN-γ when the tumor-bearing mice were treated with IL-12-transfected, non-transfected, and GFP-transfected DC, respectively (Fig.6A). Interestingly, vaccination with IL-12-producing fibroblasts also resulted in a significant although markedly lower generation of tumor-specific T cells: 550±24 pg/ml/10^6cells/36h of IFN-γ vs <20 pg/ml/10^6cells/36h in groups treated with HBSS or non-transduced fibroblasts. Similar results were obtained when the accumulation of MC38-specific T lymphocytes was determined in murine spleens (Fig.6B). The levels of MC38-induced IFN-γ in cell-free supernatants reached 8,029±56, 2,490±86, and 185±5 pg/ml/10^6cells/36h in T cell cultures obtained from mice treated with IL-12-transfected DC, IL-12-transfected fibroblasts, and GFP-transfected DC, respectively. No detectable levels of IFN-γ were assessed in all other T cell cultures. Thus, these data suggest that intraportal administration of IL-12-transfected DC caused a stimulation of immune responses and induction of systemic antitumor immunity.

Together, these results suggest that the local vaccination of liver tumor-bearing mice with DC genetically modified to overexpress IL-12 results in induction of local and systemic antitumor immune responses which was accompanied by a significant inhibition of tumor growth.

DISCUSSION

DC represent the most powerful antigen presenting cells (APC) and are therefore essential for the initiation of primary T cell responses (Steinman, 2001). Immature DC migrate from the bone marrow to the peripheral tissues where they sample the environment for foreign antigens (Shurin, 1996). Upon recognition of the antigen and activation, DC mature and migrate to draining lymph nodes in order to present the processed antigenic peptides to naïve T cells. This process is facilitated by upregulation of both co-stimulatory molecule expression and IL-12 production (Koch et al., 1996). DC represent the main source of IL-12, the most important cytokine for the induction of Th1 immune responses and regulation of the resistance to bacterial, viral, and parasitic infections, as well as to tumor growth (Esche et al., 2000b; Shurin et al., 1997a; Shurin et al., 1999b). Since Th1-biased immunity is critically important for the induction of antitumor cellular immune responses *in*

vivo, activated DC exhibit anticancer effects in part by pronounced IL-12 production, suggesting that DC are likely to be the most suitable target for therapeutic IL-12 transfection.

IL-12 comprises two disulphide-linked subunits, p40 and p35, which together form the biologically active p70 heterodimer (Esche et al., 2000b). The IL-12 receptor (IL-12R), which is expressed by natural killer (NK) cells, activated T cells, and DC, is made up of two chains IL-12Rβ1 and IL-12Rβ2 (Esche et al., 2000c). IL-12 promotes Th1 immune responses by inducing IFN-γ production and enhancing proliferation and cytotoxicity of NK and T cells (Shurin et al., 1999b). Brunda et al. initially demonstrated that IL-12 administration prolongs survival by inhibiting tumor growth and metastasis formation in mice (Brunda et al., 1993). This effect is mostly independent of NK cells but involves CD4+ and/or CD8+ T cells (Brunda et al., 1993) (Nastala et al., 1994) and eventually DC (Esche et al., 2000a). A variety of subsequent murine studies confirmed the striking antitumor effect of IL-12 (Shurin et al., 1997a). Successful approaches include administration of IL-12-transfected fibroblasts (Zitvogel et al., 1995) or tumor cells (Tahara et al., 1995), direct transfer of IL-12 cDNA via gene gun-mediated transfection of skin-tissue overlaying tumor tissue (Rakhmilevich et al., 1996), local administration of IL-12-expressing adenovirus (Caruso et al., 1996) (Bramson et al., 1996) and *in vivo* electroporation (Yamashita et al., 2001). Clinical trials have also resulted in some promising responses, although the reported toxicity limits their further development (Atkins et al., 1997; Cohen, 1995). However, locoregional delivery of IL-12 can induce immune responses without severe systemic toxicity and a very attractive option is the local administration of IL-12-transfected immune cells.

DC are ideally suited for the intratumoral administration since high numbers of tumor-associated DC (TADC) has been shown to positively correlate with a more favorable prognosis in essentially every human tumor including colon carcinoma (Schwaab et al., 2001; Shurin and Gabrilovich, 2001). Peritumoral injection of IL-12-transduced DC has been demonstrated recently to inhibit the growth of CT26 colon carcinoma in a subcutaneous murine model (Furumoto et al., 2000). However, the most common site of recurrence after hepatic resection of colorectal metastases is the residual liver metastasis (Fong, 1999). In our study, we have injected MC38 colon adenocarcinoma cells directly into the liver in order to establish colon cancer-derived liver metastases prior to using the portal vein for DC-based local administration of IL-12. The portal vein provides most of the nutrient blood flow to the normal liver (Fong, 1999). We therefore administered DC directly into the portal vein in order to develop an approach with therapeutic potential not only for macroscopic but also for occult metastases. This strategy turned out to be feasible, effective, and free of the systemic side effects. Growth of established liver metastases of colon cancer cells was significantly inhibited by a local administration of IL-12 transfected DC. This finding is in accordance with other approaches utilizing IL-12 gene therapy for experimental treatment of murine cancer (Brunda et al., 1993) (Nastala et al., 1994) (Zitvogel et al., 1995) (Tahara et al., 1995) (Rakhmilevich et al., 1996) (Caruso et al., 1996) (Bramson et al., 1996) (Yamashita et al., 2001).

The uniqueness of this study is the combined local administration of IL-12 and DC for immune gene therapy of metastatic colon cancer without addition of tumor antigen(s). Intraportal injection of DC-based vaccines is the only alternative for intratumoral administration when multiple metastasis are expected. This strategy appears to be the most physiologic since a direct application of DC into the portal vein also circumvents problems of peptide-based vaccines such as MHC restriction or antigenic heterogeneity. Importantly, the combination of a local IL-12 production with antitumor properties of DC indeed was highly beneficial since DC engineered to secrete IL-12 were significantly more efficient than non-transfected control DC in the induction of antitumor immunity in MC38-induced liver metastases model. This notion extends the recent observation of Furumoto et

al. that IL-12-transfected DC are capable of inhibiting growth of established subcutaneous tumors (Furumoto et al., 2000).

Evaluation of DC migration *in vivo* following the injection into the portal vein revealed the presence of injected DC not only in the macroscopically disease-free liver tissue but also in the spleen. In both locations accumulation peaked between 4 h and 24 h after injection with a lesser numbers at 48 h time points. Unexpectedly, significantly lower amounts of Cy3-labeled DC were detected within the liver metastases. Thus, a significant proportion of intraportally injected DC accumulates in macroscopically disease-free liver and spleen tissue for a minimum of 24 h with less amounts of DC entering the tumor tissue. This finding might indicate the existence of a potential blood-tumor barrier that eventually could represent an unidentified means of tumor-induced immunosuppression by preventing DC from entering the tumor site. Further studies are necessary to establish the underlying mechanisms of this phenomenon.

In summary, we have shown that local gene therapy with IL-12-producing DC not only inhibits growth of established MC38-derived liver metastasis but also mounts a systemic antitumor immune response *in vivo*. Clinical trials will need to evaluate the therapeutic potential of this new approach for the treatment of metastatic colorectal cancer within the liver. The newly developed approach of this study is expected to be of a particular interest in the adjuvant setting since an experimental therapy being successful in advanced metastatic disease should be even more effective against micrometastases. Finally, a local administration of IL-12-transfected DC represents a promising immunotherapeutic approach for potentially any type of metastatic cancer.

ACKNOWLEDGMENTS

This work was supported by RO1 CA80126 (to M.R.S.), RO1 CA84270 (to M.R.S.) and the Pittsburgh Foundation for Medical Research (to M.R.S.).

REFERENCES

1. Atkins M. B., Robertson M. J., Gordon M., Lotze M. T., DeCoste M., DuBois J. S., Ritz J., Sandler A. B., Edington H. D., Garzone P. D., Mier J. W., Canning C. M., Battiato L., Tahara H. and Sherman M. L. (1997) Phase I evaluation of intravenous recombinant human interleukin 12 in patients with advanced malignancies. *Clin Cancer Res* **3**, 409-17.
2. Bramson J. L., Hitt M., Addison C. L., Muller W. J., Gauldie J. and Graham F. L. (1996) Direct intratumoral injection of an adenovirus expressing interleukin- 12 induces regression and long-lasting immunity that is associated with highly localized expression of interleukin-12. *Hum Gene Ther* **7**, 1995-2002.
3. Brunda M. J., Luistro L., Warrier R. R., Wright R. B., Hubbard B. R., Murphy M., Wolf S. F. and Gately M. K. (1993) Antitumor and antimetastatic activity of interleukin 12 against murine tumors. *J Exp Med* **178**, 1223-30.
4. Caruso M., Pham-Nguyen K., Kwong Y. L., Xu B., Kosai K. I., Finegold M., Woo S. L. and Chen S. H. (1996) Adenovirus-mediated interleukin-12 gene therapy for metastatic colon carcinoma. *Proc Natl Acad Sci U S A* **93**, 11302-6.
5. Chen W., Rains N., Young D. and Stubbs R. S. (2000) Dendritic cell-based cancer immunotherapy: potential for treatment of colorectal cancer? *J Gastroenterol Hepatol* **15**, 698-705.
6. Cohen J. (1995) IL-12 deaths: explanation and a puzzle. *Science* **270**, 908.
7. Esche C., Cai Q., Peron J. M., Hunter O., Subbotin V. M., Lotze M. T. and Shurin M. R. (2000a) Interleukin-12 and Flt3 ligand differentially promote dendropoiesis in vivo. *Eur J Immunol* **30**, 2565-75.
8. Esche C., Lokshin A., Shurin G. V., Gastman B. R., Rabinowich H., Watkins S. C., Lotze M. T. and Shurin M. R. (1999a) Tumor's other immune targets: dendritic cells. *J Leukoc Biol* **66**, 336-44.
9. Esche C., Shurin M. R. and Lotze M. T. (1999b) The use of dendritic cells for cancer vaccination. *Curr Opin Mol Ther* **1**, 72-81.
10. Esche C., Shurin M. R. and Lotze M. T. (2000b) IL-12. *Cytokine Reference*, 187-201.
11. Esche C., Shurin M. R. and Lotze M. T. (2000c) IL-12 receptor. *Cytokine Reference*, 1503-1509.
12. Fong Y. (1999) Surgical therapy of hepatic colorectal metastasis. *CA Cancer J Clin* **49**, 231-55.
13. Foon K. A. (2001) Immunotherapy for colorectal cancer. *Curr Oncol Rep* **3**, 116-26.
14. Furumoto K., Arii S., Yamasaki S., Mizumoto M., Mori A., Inoue N., Isobe N. and Imamura M. (2000) Spleen-derived dendritic cells engineered to enhance interleukin-12 production elicit therapeutic antitumor immune responses. *Int J Cancer* **87**, 665-72.
15. Gambotto A., Tuting T., McVey D. L., Kovesdi I., Tahara H., Lotze M. T. and Robbins P. D. (1999) Induction of antitumor immunity by direct intratumoral injection of a recombinant adenovirus vector expressing interleukin-12. *Cancer Gene Ther* **6**, 45-53.
16. Greenlee R. T., Hill-Harmon M. B., Murray T. and Thun M. (2001) Cancer Statistics, 2001. *CA Cancer J Clin* **51**, 15-36.
17. Hewitt P. M., Dwerryhouse S. J., Zhao J. and Morris D. L. (1998) Multiple bilobar liver metastases: cryotherapy for residual lesions after liver resection. *J Surg Oncol* **67**, 112-6.
18. Koch F., Stanzl U., Jennewein P., Janke K., Heufler C., Kampgen E., Romani N. and Schuler G. (1996) High level IL-12 production by murine dendritic cells: upregulation via MHC class II and CD40 molecules and downregulation by IL-4 and IL-10. *J Exp Med* **184**, 741-6.
19. Morse M. A., Nair S., Fernandez-Casal M., Deng Y., St Peter M., Williams R., Hobeika A., Mosca P., Clay T., Cumming R. I., Fisher E., Clavien P., Proia A. D., Niedzwiecki D., Caron D.

and Lyerly H. K. (2000) Preoperative mobilization of circulating dendritic cells by Flt3 ligand administration to patients with metastatic colon cancer. *J Clin Oncol* **18**, 3883-93.
20. Nastala C. L., Edington H. D., McKinney T. G., Tahara H., Nalesnik M. A., Brunda M. J., Gately M. K., Wolf S. F., Schreiber R. D., Storkus W. J. and et al. (1994) Recombinant IL-12 administration induces tumor regression in association with IFN-gamma production. *J Immunol* **153**, 1697-706.
21. Pirtskhalaishvili G., Shurin G. V., Esche C., Cai Q., Salup R. R., Bykovskaia S. N., Lotze M. T. and Shurin M. R. (2000a) Cytokine-mediated protection of human dendritic cells from prostate cancer-induced apoptosis is regulated by the Bcl-2 family of proteins. *Br J Cancer* **83**, 506-13.
22. Pirtskhalaishvili G., Shurin G. V., Gambotto A., Esche C., Wahl M., Yurkovetsky Z. R., Robbins P. D. and Shurin M. R. (2000b) Transduction of dendritic cells with Bcl-xL increases their resistance to prostate cancer-induced apoptosis and antitumor effect in mice. *J Immunol* **165**, 1956-64.
23. Radinsky R. and Ellis L. M. (1996) Molecular determinants in the biology of liver metastasis. *Surg Oncol Clin N Am* **5**, 215-29.
24. Rakhmilevich A. L., Turner J., Ford M. J., McCabe D., Sun W. H., Sondel P. M., Grota K. and Yang N. S. (1996) Gene gun-mediated skin transfection with interleukin 12 gene results in regression of established primary and metastatic murine tumors. *Proc Natl Acad Sci U S A* **93**, 6291-6.
25. Schwaab T., Weiss J. E., Schned A. R. and Barth R. J., Jr. (2001) Dendritic cell infiltration in colon cancer. *J Immunother* **24**, 130-7.
26. Shurin M. R. (1996) Dendritic cells presenting tumor antigen. *Cancer Immunol Immunother* **43**, 158-64.
27. Shurin M. R., Esche C., Lokshin A. and Lotze M. T. (1999a) Apoptosis in Dendritic Cells. In *Dendritic Cells: Biology and Clinical Applications* (Edited by M.T.Lotze and A.W.Thomson), p. 673-692. Academic Press, San Diego.
28. Shurin M. R., Esche C., Peron J. M. and Lotze M. T. (1997a) Antitumor activities of IL-12 and mechanisms of action. *Chem Immunol* **68**, 153-74.
29. Shurin M. R. and Gabrilovich D. I. (2001) Regulation of Dendritic Cell System by Tumor. *Cancer Research Therapy and Control* **11**, 65-78.
30. Shurin M. R., Kirkwood J. M. and Esche C. (2000) Cytokine-based therapy for melanoma: pre-clinical studies. *Forum (Genova)* **10**, 204-26.
31. Shurin M. R., Lu L., Kalinski P., Stewart-Akers A. M. and Lotze M. T. (1999b) Th1/Th2 balance in cancer, transplantation and pregnancy. *Springer Semin Immunopathol* **21**, 339-59.
32. Shurin M. R., Pandharipande P. P., Zorina T. D., Haluszczak C., Subbotin V. M., Hunter O., Brumfield A., Storkus W. J., Maraskovsky E. and Lotze M. T. (1997b) FLT3 ligand induces the generation of functionally active dendritic cells in mice. *Cell Immunol* **179**, 174-84.
33. Steinman R. M. (2001) Dendritic cells and the control of immunity: enhancing the efficiency of antigen presentation. *Mt Sinai J Med* **68**, 106-66.
34. Tahara H., Zitvogel L., Storkus W. J., Zeh H. J., 3rd, McKinney T. G., Schreiber R. D., Gubler U., Robbins P. D. and Lotze M. T. (1995) Effective eradication of established murine tumors with IL-12 gene therapy using a polycistronic retroviral vector. *J Immunol* **154**, 6466-74.
35. Yamashita Y. I., Shimada M., Hasegawa H., Minagawa R., Rikimaru T., Hamatsu T., Tanaka S., Shirabe K., Miyazaki J. I. and Sugimachi K. (2001) Electroporation-mediated interleukin-12 gene therapy for hepatocellular carcinoma in the mice model. *Cancer Res* **61**, 1005-12.
36. Zitvogel L., Tahara H., Robbins P. D., Storkus W. J., Clarke M. R., Nalesnik M. A. and Lotze M. T. (1995) Cancer immunotherapy of established tumors with IL-12. Effective delivery by genetically engineered fibroblasts. *J Immunol* **155**, 1393-403.

FIGURE LEGENDS

Figure 1. IL-12-transfected DC and fibroblasts produce high levels of IL-12 protein in cultures. Bone marrow-derived DC and MF57B$^-$ fibroblast cell line were transfected with adenovector encoding murine IL-12 gene as described in Material and Methods. Production of mIL-12 p70 in cell-free supernatant was measured using ELISA according to the manufacturer's instructions. The average ± SEM from three independent experiments is shown. DC, non-transfected DC; DC/GFP, DC transfected with GFP gene; DC/IL12, DC transfected with *m*IL-12 gene; FIB, a murine fibroblast cell line; FIB/IL12, fibroblasts transfected with *m*IL-12 gene. *, $p<0.001$.

Figure 2. IL-12-transfected DC expressed higher levels of co-stimulatory and CD40 molecules. Bone marrow-derived DC were transfected with adenovector encoding murine IL-12 gene as described in Material and Methods. The expression of cell surface molecules on transfected and control cell cultures was assessed by FACScan analysis. X axis, mean fluorescent intensity for CD80-FITC, CD86-FITC or CD40-FITC; Y axis, mean fluorescent intensity for CD11c-PE; DC, non-transfected cells; DC/LacZ, DC transfected with LacZ gene; DC/IL12, DC transfected with IL-12 gene.

Figure 3. Intraportal administration of IL-12-transfected DC inhibits growth of established colon adenocarcinoma in the liver. Five x 10^5 MC38 colon cancer cells were injected under the capsule of the left medial liver lobe in mice on Day 1 and different cellular vaccines were administered into the portal vein on Day 7. Mice were sacrificed on Day 21 and liver metastases were measured as described in Materials and Methods. Each bar represents the mean ± SEM from three independent experiments. HBSS, Hanks solution; DC, non-transfected DC; DC/GFP, DC transfected with GFP gene; DC/IL12, DC transfected with *m*IL-12 gene; FIB, a murine fibroblast cell line; FIB/IL12, fibroblasts transfected with *m*IL-12 gene. * $p < 0.05$ vs control; **, $p<0.0001$ vs FIB/IL-12 group.

Figure 4. Distribution of Cy3-labeled DC injected into the portal vein in liver tumor-bearing mice. Cultured bone marrow-derived DC were labeled with Cy3, a water-soluble cyanine dye (1 μg/ml, 37°C, 30 min), washed, and injected into the portal vein of liver tumor-bearing mice as described in Materials and Methods. The livers (**a**, **b**, **c**), spleens (**d**, **e**, **f**), and tumors (**g**, **h**, **i**) were collected 4 h (**a**, **d**, **g**), 24 h (**b**, **e**, **h**), and 48 h (**c**, **f**, **i**) later and the presence of Cy3-positive cells was determined by the confocal microscopy. Analysis of tissues obtained from animals treated with non-labeled DC served as a negative control and demonstrated no significant fluorescence.

Figure 5. Direct administration of IL-12-transfected DC into the portal vein results in accumulation of immune cells in the liver metastasis. Cultured bone marrow-derived DC were transfected with IL-12 gene (**a**, **c**, **e**) or GFP gene (**b**, **d**, **f**) and injected into the portal vein in mice having 7-day old colon adenocarcinoma in the liver. Tumor tissues were collected two weeks later and evaluated for the presence of CD4+ (**a**, **b**), NLDC145+ (**c**, **d**), and CD8+ (**e**, **f**) cells by immunohistochemistry as described in Materials and Methods. Analysis of tumor infiltrating cells in animals treated with non-transfected DC, HBSS, or fibroblasts revealed no significant differences when compared with animals treated with GFP-transfected DC (data not shown). Negative controls

comprised of tissue samples stained with only secondary antibody showed no positive staining. Magnification 400X.

Figure 6. Induction of systemic antitumor immune responses by a single intraportal injection of IL-12-transfected DC in liver tumor-bearing mice. Bone marrow-derived DC and MF57B$^-$ fibroblast cell line were transfected with adenovector encoding murine IL-12 gene as described in Material and Methods. Transfected and control cells were injected into the portal vein 7 days after inoculation of MC38 tumor cells under the liver capsule. Splenic and lymph node T cells were harvested two weeks later and stimulated with irradiated MC38 cells. Cell-free supernatants were collected and the production of IFN-γ was assessed by ELISA. HBSS, Hanks solution; DC, non-transfected DC; DC/GFP, DC transfected with GFP gene; DC/IL12, DC transfected with *m*IL-12 gene; FIB, a murine fibroblast cell line; FIB/IL12, fibroblasts transfected with *m*IL-12 gene. * $p < 0.001$ vs HBSS group.

Table I. Distribution of Cy3-labeled DC in the tumor, liver, spleen and draining lymph nodes after administration into the portal vein (Portal) or vena cava (IVC)

	Tumor		Liver		Spleen		LN	
Time after injection	**Portal**	**IVC**	**Portal**	**IVC**	**Portal**	**IVC**	**Portal**	**IVC**
4 h	-*	-	+++	+	+++	+++	-	-
24 h	+	-	+++	++	+++	+++	++	+
48 h	-	-	++	++	++	++	-	++

* The number of Cy3-positive cells in tissues was determined semiquantitatively by the confocal microscopy and expressed as: "-", no positive cells; "+", 1-5 positive cells/field; "++", 6-10 positive cells/field; "+++", ≥ 11 positive cells/field. No fluorescence was detected in control tissues obtained from animals receiving non-labeled cells.

Table II. Immunohistochemical evaluation of T cells and DC in the tumor and spleen tissues

Staining	Treatment groups					
	HBSS* Tumor/spleen	FIB Tumor/spleen	DC Tumor/spleen	DC/GFP Tumor/spleen	FIB/IL12 Tumor/spleen	DC/IL12 Tumor/spleen
CD4	-/++**	±/++	-/++	-/++	±/++	++/+++
CD8	-/±	±/+	±/+	±/+	±/+	++/+
DC	+/±	±/±	+/±	+/±	+/±	++/±
Neg	-/-	-/-	-/-	-/-	-/-	-/-

** The number of positive cells in tumor/spleen tissues was determined semiquantitatively and expressed as: "-", no positive staining; "±", weak positive staining with <5% of the cells being positive; "+", positive staining with <10% of positive cells; "++", moderate positive staining with <25% of positive cells; "+++", strong positive staining with >25% of positive cells. Tissue staining with only secondary antibody served as a negative control. Freshly isolated splenocytes and cultured bone marrow-derived DC were used as positive controls.

* HBSS, Hanks solution; DC, non-transfected DC; DC/GFP, DC transfected with GFP gene; DC/IL12, DC transfected with *m*IL-12 gene; FIB, murine fibroblast cell line 3T3; FIB/IL12, fibroblasts transfected with *m*IL-12 gene.

Table III. The effect of DC-based intraportal vaccinations on the plasma levels of IL-12 and IFN-γ in mice bearing MC38 colon adenocarcinoma in the liver

Vaccine	Time after administration	Plasma cytokines, pg/ml		
		IL-12*	IFN-γ	IL-4
DC/IL12**	4 h	ND***	ND	ND
	24 h	ND	60.5±3.2	ND
	48 h	265.7±9.6	185.8±4.6	ND
	72 h	ND	ND	ND
DC/GFP	4-72 h	ND	ND	ND
DC	4-72 h	ND	ND	ND
HBSS	4-72 h	ND	ND	ND

* Plasma samples were prepared from blood obtained by heart puncture at various time-points following the intraportal administration of different DC-based vaccines. Cytokine levels were determined by ELISAs and expressed as mean ± SEM from three independent experiments.

** HBSS, Hanks solution; DC, non-transfected DC; DC/GFP, DC transfected with GFP gene; DC/IL12, DC transfected with *m*IL-12 gene.

*** ND, non-detectable. Concentration of cytokines in the samples was lower than the sensitivity of the ELISA kit (<20 pg/ml).

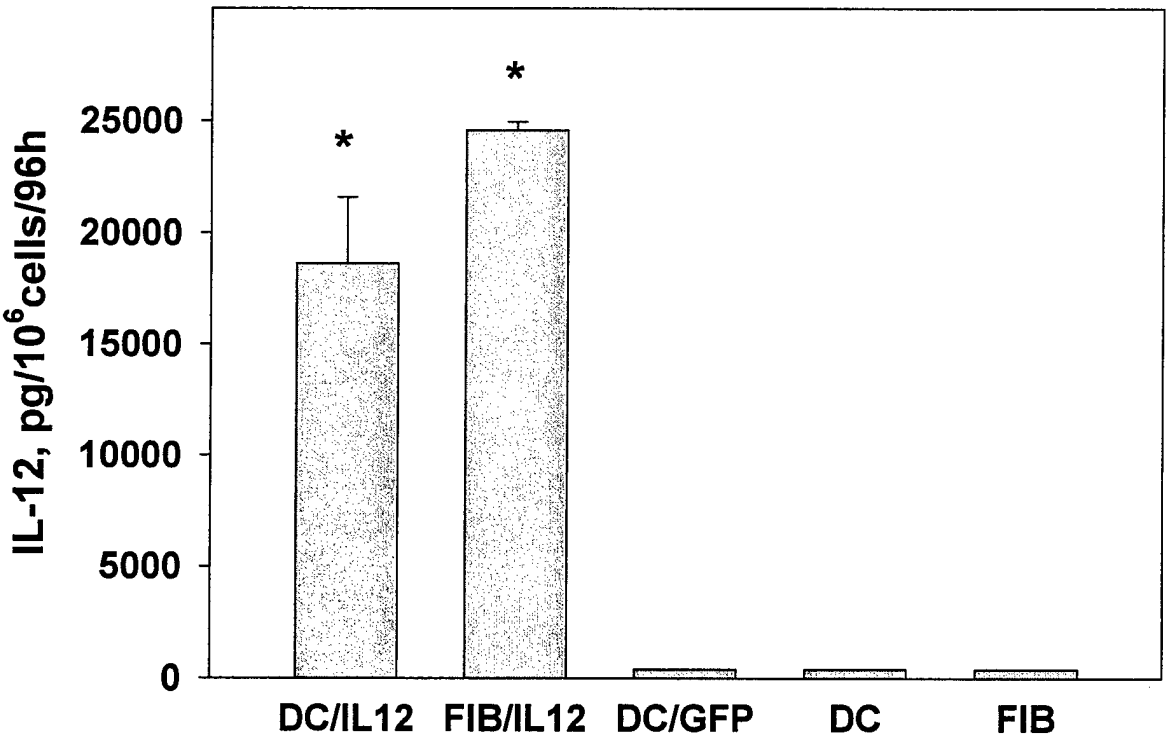
IL-12, pg/10^6cells/96h
25000
20000
15000
10000
5000
0
*
*
DC/IL12
FIB/IL12
DC/GFP
DC
FIB

Figure 1

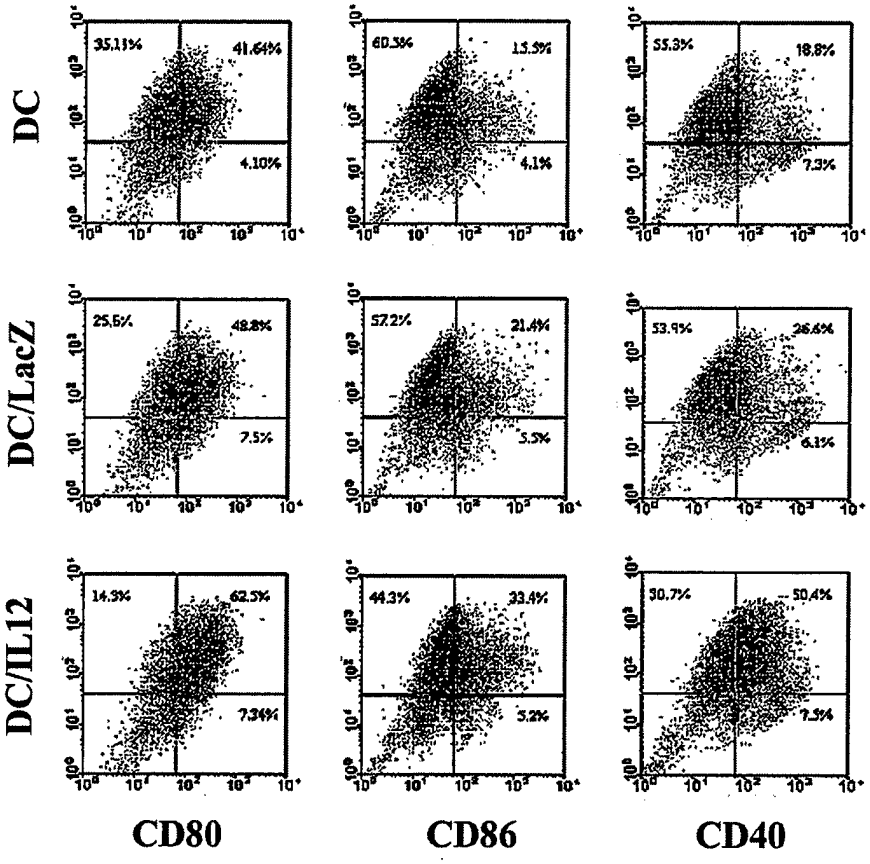
DC
DC/LacZ
DC/IL12
35.11%
41.64%
4.10%
60.5%
15.5%
4.1%
55.3%
18.8%
7.3%
25.6%
48.8%
7.5%
57.2%
21.4%
5.5%
53.9%
26.6%
6.1%
14.3%
62.5%
7.34%
44.3%
33.4%
5.2%
50.7%
30.4%
7.5%
CD80
CD86
CD40

Figure 2

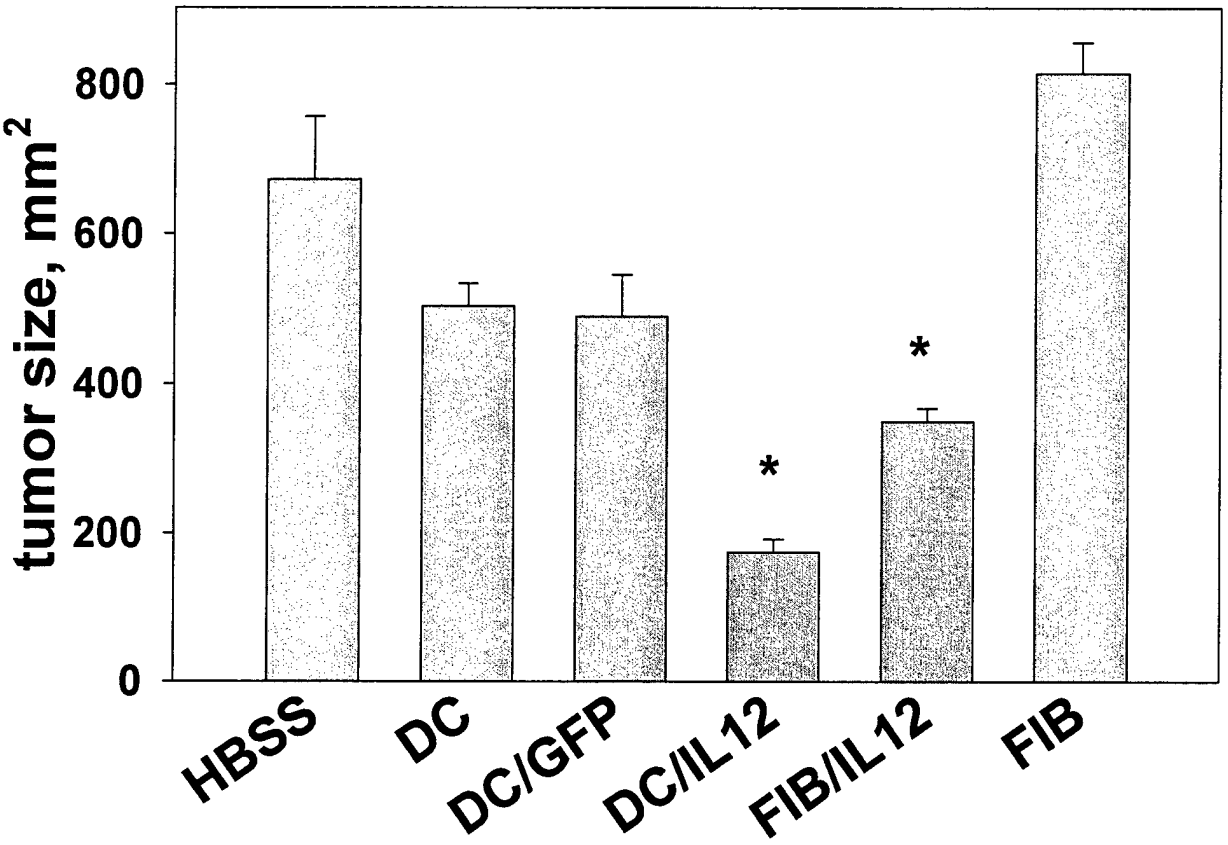
tumor size, mm2
800
600
400
200
0
*
*
HBSS
DC
DC/GFP
DC/IL12
FIB/IL12
FIB

Figure 3

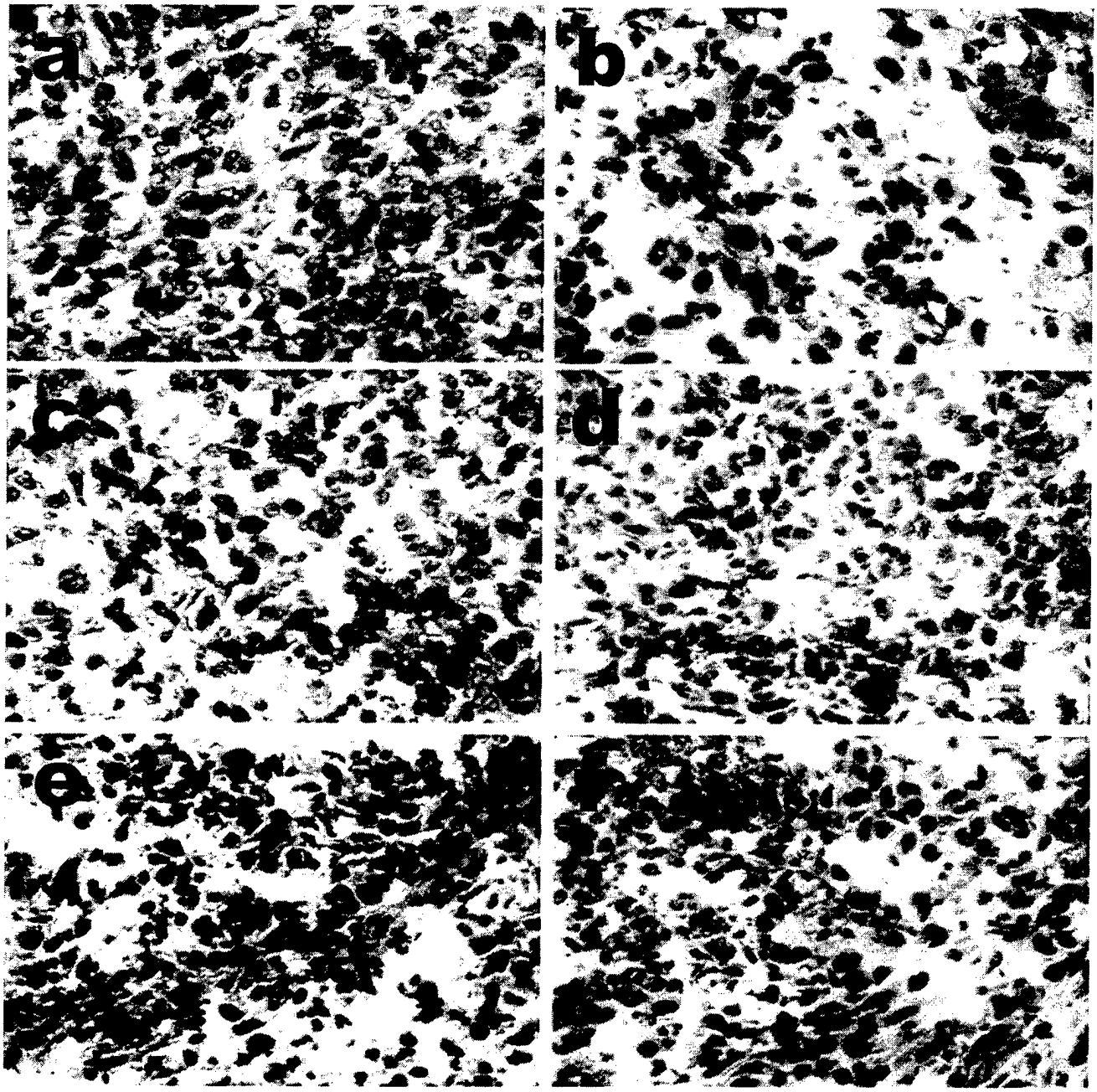

Figure 4

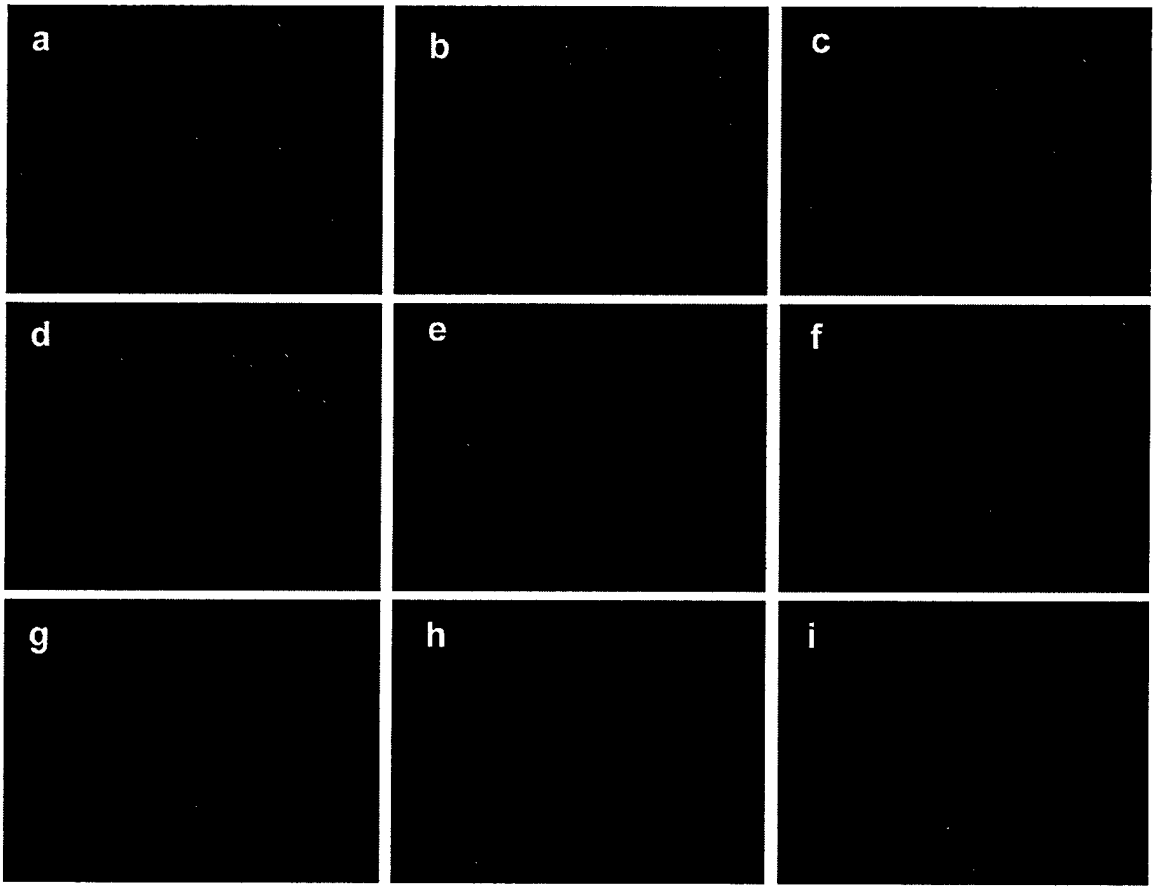

Figure 5

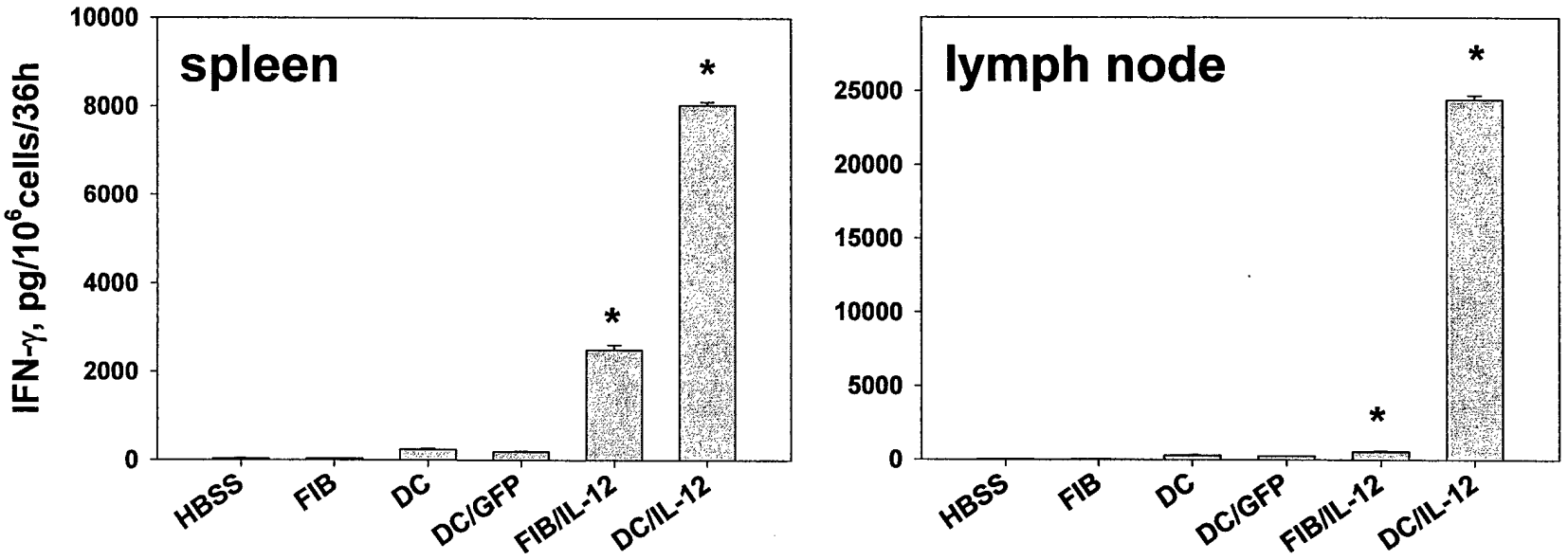
spleen
lymph node
IFN-γ, pg/10^6cells/36h
10000
8000
6000
4000
2000
0
25000
20000
15000
10000
5000
0
*
HBSS
FIB
DC
DC/GFP
FIB/IL-12
DC/IL-12

Figure 6